

State of Oregon
Oregon Department of Geology and Mineral Industries
Vicki S. McConnell, State Geologist

OPEN-FILE REPORT O-13-08

Landslide Hazard and Risk Study of Northwestern Clackamas County, Oregon

by William J. Burns¹, Katherine A. Mickelson¹, Cullen B. Jones¹, Sean G. Pickner¹,
Kaleena L. B. Hughes¹, and Rachel Sleeter²



2013

NOTICE

This product is for informational purposes and may not have been prepared for or be suitable for legal, engineering, or surveying purposes. Users of this information should review or consult the primary data and information sources to ascertain the usability of the information. This publication cannot substitute for site-specific investigations by qualified practitioners. Site-specific data may give results that differ from the results shown in the publication.

Oregon Department of Geology and Mineral Industries Open-File Report O-13-08
Published in conformance with ORS 516.030

For copies of this publication or other information about Oregon's geology and natural resources, contact:

Nature of the Northwest Information Center
800 NE Oregon Street #28, Suite 965
Portland, Oregon 97232
(971) 673-2331
<http://www.naturenw.org>

For additional information:
Administrative Offices
800 NE Oregon Street #28, Suite 965
Portland, OR 97232
Telephone (971) 673-1555
Fax (971) 673-1562
<http://www.oregongeology.org>
<http://egov.oregon.gov/DOGAMI/>

TABLE OF CONTENTS

1.0 SUMMARY	1
2.0 INTRODUCTION	1
3.0 STUDY AREA	3
4.0 PREVIOUS WORK	5
5.0 METHODS	5
5.1 Assets	5
5.1.1 Permanent population.....	5
5.1.2 Buildings and land	7
5.1.3 Critical facilities and primary infrastructure	8
5.2 Landslide hazards	9
5.2.1 Landslide inventory.....	10
5.2.2 Shallow-landslide susceptibility	10
5.2.3 Deep-landslide susceptibility	11
5.2.3.1 <i>High-susceptibility zone</i>	12
5.2.3.2 <i>Head scarp–flank polygons and buffers</i>	13
5.2.3.3 <i>Moderate susceptibility zone</i>	14
5.2.3.4 <i>Combined moderate factors score</i>	21
5.2.3.5 <i>Minimal landslide deposits and head scarp–flank buffers</i>	22
5.2.3.6 <i>Delineation of the moderate susceptibility zone</i>	22
5.2.3.7 <i>Final deep-landslide susceptibility zones</i>	23
5.2.3.8 <i>Deep-landslide susceptibility map</i>	24
5.3 Risk Analysis and Loss Estimation	25
5.3.1 Exposure analysis.....	25
5.3.2 Hazus-MH analysis.....	26
5.3.3 Historic landslide data and loss estimation.....	28
6.0 RESULTS	29
6.1 Permanent population results	29
6.2 Buildings and land results	29
6.3 Critical facilities and primary infrastructure results	30
6.4 Landslide inventory results	31
6.5 Shallow-landslide susceptibility results	33
6.6 Deep-landslide susceptibility results	33
6.7 Risk analysis and loss estimation results	34
6.7.1 Exposure analysis results.....	34
6.7.2 Hazus-MH analysis results.....	35
7.0 DISCUSSION AND CONCLUSIONS	36
8.0 ACKNOWLEDGMENTS	37
9.0 REFERENCES	37

LIST OF FIGURES

Figure 1.	Study area location map (outlined in black)	1
Figure 2.	January 2009 landslide events in northwestern Clackamas County	2
Figure 3.	Map of the study area showing Counties, cities, and communities	3
Figure 4.	Index map of previously published landslide inventory maps for the study area.	4
Figure 5.	Permanent population in the study area.	6
Figure 6.	Buildings and land in the study area.	7
Figure 7.	Critical facilities and primary infrastructure	8
Figure 8.	New digital surficial geology/material properties map	11
Figure 9.	Example of a lidar-based landslide inventory map and example map showing deep landslide deposits converted to high susceptibility zone.	12
Figure 10.	Diagram of the 2H:1V head scarp buffer	13
Figure 11.	Diagram of the 2 horizontal to 1 vertical ratio.	13
Figure 12.	Head scarp retrogression buffer.	14
Figure 13.	Example of buffered deep landslide head scarp-flank polygons converted to high susceptibility zone	14
Figure 14.	Engineering geology map of the Oregon City portion of the study area.	15
Figure 15.	Landslides in each geologic unit in the study area	16
Figure 16.	Frequency data summary statistics	16
Figure 17.	Map of susceptible geologic units factor.	16
Figure 18.	Map of the contact between Boring Lava Troutdale Formations showing landslide deposits and landslides that touch and are along the contact.	17
Figure 19.	Map of minimum bounding geometry rectangles derived from landslide polygons and summary statistics of the MBG width of these landslides.	17
Figure 20.	Map of the susceptible contact factor	18
Figure 21.	Map of the mean slope angle of each engineering geology polygon derived from the landslides located within each polygon	19
Figure 22.	Map of the susceptible slopes factor	19
Figure 23.	Maps of interpolated landslide direction of movement and slope aspect derived from the lidar DEM	20
Figure 24.	Map of the susceptible preferred direction factor	21
Figure 25.	Map of the combined moderate factor scores.	21
Figure 26.	Maps of minimal moderate susceptibility zone and landslide deposits and of the high-susceptibility zone, the combined moderate factors score, the minimal moderate zone, and the delineated line between the moderate and the low susceptibility zones.	22
Figure 27.	Map of deep landslide susceptibility zones	23
Figure 28.	Example of the deep landslide susceptibility map of the northwest quarter of the Oregon City quadrangle, Clackamas County, Oregon	24
Figure 29.	Map of the 60 selected census tracts used in the Hazus-MH analysis.	26
Figure 30.	Landslide susceptibility map ranging from 0 to 10 of the Hazus-MH study extent	28
Figure 31.	Overview map of the landslide inventory.	31
Figure 32.	Graph of historic landslides grouped into 5-year bins	32
Figure 33.	Photographs of historic landslide damage in Oregon City	32

LIST OF TABLES

Table 1.	Geotechnical material properties	10
Table 2.	Final hazard zone matrix	23
Table 3.	Communities for exposure reporting	25
Table 4.	Landslide susceptibility of geologic groups	27
Table 5.	Hazus-MH analyses	27
Table 6.	Permanent population by community	29
Table 7.	Building and land inventory summary	29
Table 8.	Critical facilities inventory summary	30
Table 9.	Roads and electric system inventory summary	30
Table 10.	Summary of the northwestern Clackamas County landslide inventory	31
Table 11.	Summary of shallow-landslide susceptibility hazard zones by community	33
Table 12.	Summary of deep-landslide susceptibility hazard zones by community	33
Table 13.	Summary of exposure of select assets to the three landslide inventory hazard zones	34
Table 14.	Summary of the six landslide susceptibility hazard zones and study area wide exposure of select assets	34
Table 15.	Summary of Hazus-MH results	35

MAP PLATES

Plate 1. Asset overview maps of northwestern Clackamas County, Oregon: primary infrastructure, population density, and generalized land use

Plate 2. Landslide inventory and shallow- and deep-landslide susceptibility overview maps of northwestern Clackamas County, Oregon

Plates 3–73 (odd numbers): Detailed shallow landslide susceptibility maps for NE, NW, SE, and SW quarter-quadrangle extents in the Canby, Damascus, Estacada, Gladstone, Lake Oswego, Oregon City, Redland, Sandy, and Sherwood U.S. Geological Survey 7.5-minute quadrangles

Plates 4–74 (even numbers): Detailed deep landslide susceptibility maps for NE, NW, SE, and SW quarter-quadrangle extents in the Canby, Damascus, Estacada, Gladstone, Lake Oswego, Oregon City, Redland, Sandy, and Sherwood U.S. Geological Survey 7.5-minute quadrangles

DIGITAL APPENDICES

Contents of the appendices are listed here. See the Appendices folder on the CD-ROM for files.

Appendix A. Generalized Zoning/Land Use/FEMA Hazus-MH Occupancy Relationship	Building_Attribution_Method.docx Tax_Lots_to_HAZUS_Occupancy_Class_Method_and_Crosswalk_Table.docx
Appendix B. DOGAMI Special Paper 42, Protocol for Inventory Mapping of Landslide Deposits from Light Detection and Ranging (Lidar) Imagery - report text only	DOGAMI-Special Paper-42-report-text-only.pdf
Appendix C. DOGAMI Special Paper 45, Protocol for shallow-landslide susceptibility mapping - report text only	DOGAMI-Special Paper-45-report-text-only.pdf
Appendix D. Geotechnical Material Properties	Geotechnical_Data.xlsx Reference_List_for_Geotechnical_Data.docx
Appendix E. Deep-Landslide Susceptibility GIS Method Details	Deep-Landslide_Susceptibility_GIS_Method_Details.docx
Appendix F. Exposure Analysis Process and Results Details	Exposure_Analysis_GIS_Processes.docx Exposure_Analysis_Results.xlsx
Appendix G. Historic Landslide Data	Historic_Landslides_in_NW_Clackamas_County.pdf Historic_Landslides_in_NW_Clackamas_County.xlsx
Appendix H. Hazus-MH Summary Reports	Cascadia_M9.0_earthquake_with_landslide_hazard.pdf Cascadia_M9.0_earthquake_with_no_landslide_hazard.pdf Crustal_Portland_Hills_M6.8_earthquake_with_landslide_hazard_set_to_9_out_of_10.pdf Crustal_Portland_Hills_M6.8_earthquake_with_landslide_hazard.pdf Crustal_Portland_Hills_M6.8_earthquake_with_no_landslide_hazard.pdf

GEOGRAPHIC INFORMATION SYSTEM (GIS) DATA

Geodatabases are in Esri v10.1 format.

Landslide Inventory Geodatabase:	Clackamas_landslides_10_1.gdb: feature classes: Deposits (polygons), Photos (points), Scarp_Flanks (polygons), Scarps (polylines)
Shallow-Landslide Susceptibility Geodatabase:	Shallow_Landslide_Suceptibility_Clackamas_10_1.gdb: shallow_landslide_susceptibility feature class (polygons)
Deep-Landslide Susceptibility Geodatabase:	Deep_Landslide_Susceptibility_Clackamas_10_1.gdb: deep_landslide_susceptibility feature class (polygons)
Assets Geodatabase:	Clackamas_Assets10_.gdb: feature classes: Building_Critical_Facilities (polygons), Buildings (polygons), clasck07da2_PopulationDensity (raster), Dam_Electric (polygons), major_substations (polygons), major_transmission_towers (points), Metro_Boundary (polygons), railroads (polylines), Study-Extent_wCities (polygons)

1.0 SUMMARY

Northwestern Clackamas County has significant landslide hazards in some of the most developed land in Oregon. The intersection of landslide hazard and dense development result in a relatively high level of risk. We performed this study to increase understanding of the landslide hazard and risk, so that targeted risk reduction could be continued and accelerated.

We found 370 historic landslides occurred in the study area during the period 1964–2009. We estimated annual direct losses from these landslides ranged from hundreds of thousands to millions of dollars for typical winter storm years in Oregon, and up to tens of millions to \$75 million in severe storm years, such as 1996.

A major part of this study was developing the lidar-based landslide inventory and shallow- and deep-landslide susceptibility maps. We mapped 2,885 existing landslides, which cover roughly 7% of the study area. Many of these are prehistoric or ancient landslides (that is, older than 150 years); however, these landslides should be considered just barely stable and in most cases would require only a small change in stability to reactivate. We found the large, deep landslides are a primary threat in the study area. Asset exposure to these large, deep landslides is significant — more than 7,000 residents and more than 3,000 buildings with a combined land and building value of \$832 million are located on large, deep landslides. Damage and losses alone from landslides induced by a local large crustal earthquake may be in the range of \$1 billion with ~4,500 buildings moderately to completely destroyed.

The next step after identifying hazard and risk is to work on landslide risk reduction. The three primary actions are 1) awareness, 2) regulation, and 3) planning. Making everyone aware of the hazard and associated risk is the first step, so that everyone can work on risk reduction. Fliers can be made available on websites and/or distributed to help educate land owners of activities individuals can work on to reduce landslide risk.

The landslide inventory and susceptibility maps produced as part of this project show areas of low, moderate, and high potential for landslides in the future and are suited for use in connection with landslide ordinances or building code regulation. The maps could also be used in short- and long-term development planning, comprehensive planning, and maintenance planning.

2.0 INTRODUCTION

Northwestern Clackamas County is plagued with landslide disasters. Not only is the landslide hazard high and extensive, but portions of the county are some of the most densely developed parts of Oregon (Figure 1). The high landslide hazard combined with dense development results in high risk and thus the primary reason for this study.



Figure 1. Study area location map (outlined in black).

The Federal Emergency Management Agency (FEMA) issued 28 major disaster declarations for Oregon for the period 1955–2012. Most of these are related to storm events that caused flooding and, commonly, landslides. During this time, at least six Presidential Disaster Declarations for Clackamas County noted landslides as part of the reason for the declaration (FEMA, 2012a):

- 1964 – FEMA DR184, Heavy Rains and Flooding
- 1996 – FEMA DR1099, Oregon Severe Storms/ Flooding, estimated \$50 million in damage from flood and landslides. Directly or indirectly affected three-quarters of the county’s residents
- 2003-2004 – FEMA DR1510, Severe Winter Storms, County received \$183,000
- 2005-2006 – FEMA DR1632, Oregon Severe Storms, Flooding, Landslides, and Mudslides, county received \$245,000
- 2009 – FEMA DR1824, Severe Winter Storm, Record and Near Record Snow, Landslides, and Mudslides, preliminary countywide per capita impact \$3.33
- 2011 – FEMA DR1956-DR, Severe Winter Storm, Flooding, Mudslides, Landslides, and Debris Flows, preliminary countywide per capita impact \$12

FEMA DR1824 was declared after the January 2009 severe storm. Much of northwestern Oregon experienced flooding and landslides. Many landslides occurred in Clackamas County, impacting infrastructure and homes. Several homes were completely destroyed in this event (Figure 2). Clackamas County submitted a mitigation planning grant proposal to FEMA. That proposal was accepted and was funded through the FEMA Hazard Mitigation Grant Program. This DOGAMI project, completed between 2012 and 2013, is partially funded by that grant.

The main purpose of this project is to help communities in this region become more resilient to landslide hazards by providing accurate, detailed, and up to date information about these hazards and community assets at risk.

The main objectives of this study are to:

- compile and incorporate existing data including previous geologic hazard reports and the county natural hazard mitigation plans
- create new databases of landslide hazards including landslide inventory and susceptibility
- compile and/or create a database of critical facilities and primary infrastructure, generalized land occupancy (land use/zoning), buildings, and population distribution data
- perform exposure and Hazus-MH–based risk analysis
- share the results through this report

The body of this report describes the methods and results for these objectives.



Figure 2. (left) Photograph showing a landslide in Paradise Park off Heiple Road that pushed a home off its foundation; the home then caught fire. (right) Photograph showing a landslide from Greenbluff Drive that slid down and through a home on Woodhurst Place. Both landslides occurred during January 2009 in northwestern Clackamas County.

3.0 STUDY AREA

The study covers an area of approximately 375 square miles in Clackamas County and includes small parts of Multnomah and Washington Counties. It is geographically bounded by the Willamette River Valley to the west and the Cascade Mountains to the east (Figure 3). The communities include the entire extents of Barlow, Canby, Damascus, Estacada, Gladstone, Happy Valley, Johnson City, Lake Oswego, Milwaukie, Oregon City, Sandy, West Linn, Wilsonville, and portions of unincorporated Clackamas County, Tualatin, River Grove, and Portland (Figure 3). For this study we combined the five small cities and/

or portions of cities into a single “other jurisdiction” category, mostly because the communities were only very small pieces or small entities. The combined communities include Barlow, Johnson City, Rivergrove, Tualatin, and Portland. We also included the Metro urban growth boundary as a community boundary in our analysis (green line on Figure 3). Metro is the regional government for the Portland metropolitan area. Oregon law requires each city or metropolitan area in the state to have an urban growth boundary that separates urban land from rural land. Metro is responsible for managing the Portland metropolitan region’s urban growth boundary (<http://www.oregonmetro.gov/index.cfm/go/by.web/id=277>).

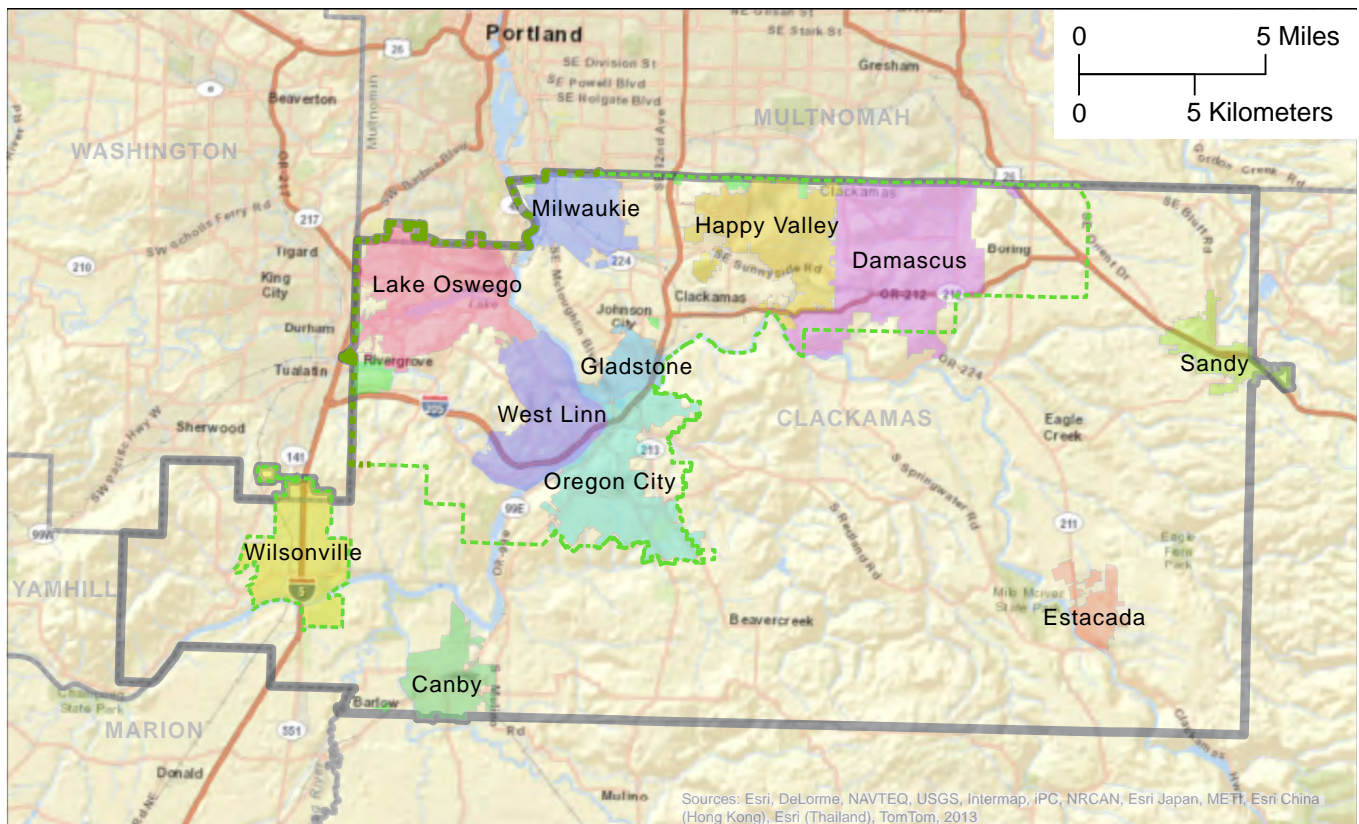
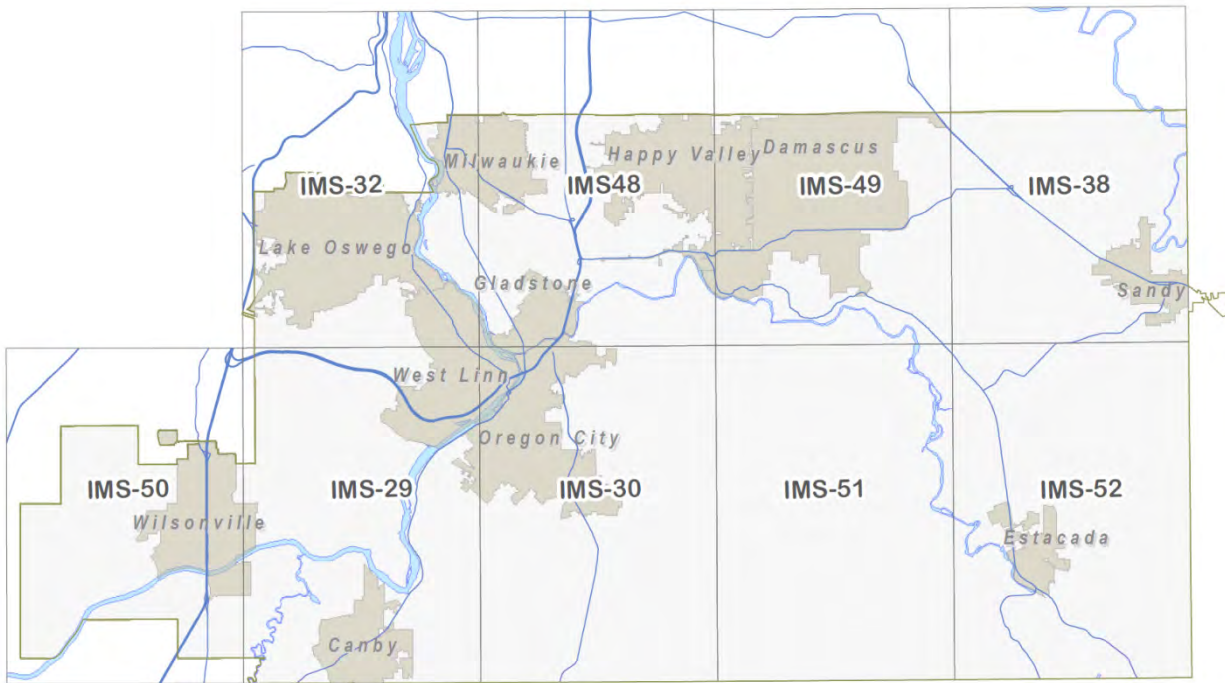


Figure 3. Map of the study area showing counties, cities, and communities. The dashed green line indicates the Metro urban growth boundary.

The geology, topography, and climate of the study area are all conducive to landslide hazards. An overview of the bedrock geology is provided in DOGAMI Bulletin 99 (Schlicker and Finlayson, 1979). The surficial geology was recently mapped and described in DOGAMI Open-File Report O-12-02 (Ma and others, 2012), and landslide inventory for all of the area was completed and published as DOGAMI Interpretive Maps IMS-29, -30, -32, -38, -48, -49, -50, -51, and -52 (Figure 4).



- IMS-29, Canby quadrangle (Burns, 2009)
- IMS-30, Oregon City quadrangle (Burns and Mickelson, 2010)
- IMS-32, Lake Oswego quadrangle (Burns and Duplantis, 2010)
- IMS-38, Sandy quadrangle (Burns and others, 2012a)
- IMS-48, Gladstone quadrangle (Burns and others, 2012b)
- IMS-49, Damascus quadrangle (Burns and others, 2012c)
- IMS-50, Sherwood quadrangle (Burns and others, 2012d)
- IMS-51, Redland quadrangle (Burns and others, 2012e)
- IMS-52, Estacada quadrangle (Burns, 2012f)

Figure 4. Index map of previously published DOGAMI landslide inventory maps for the study area. All maps are at scale 1:8,000.

4.0 PREVIOUS WORK

A number of previous geologic and geologic hazard studies have been conducted in or near the study area. We reviewed this body of work to assess the mapped hazards so we could decide if we needed to construct new data or redelineate the existing data. Among DOGAMI recently acquired very detailed topographic data derived from lidar, airborne laser scanning data that produces digital elevation models (DEMs) with a nominal resolution of 3 ft. The new lidar topography allows us to remap landslide and flood hazards with significantly greater accuracy (Burns, 2007). The previous studies we reviewed include:

- DOGAMI Bulletin 99 (Schlicker and Finlayson, 1979)
- DOGAMI Open-File Report O-12-02 surficial geology (Ma and others, 2012)
- DOGAMI IMS- IMS-29, 30, 32, 38, 48, 49, 50, 51, and 52 New Landslide Maps
- Clackamas County Natural Hazard Mitigation Plan (<http://www.clackamas.us/emergency/naturalhazard.html>)
- Statewide Landslide Information Database for Oregon (SLIDO), release 2 (Burns and others, 2011)
- Oregon Geologic Data Compilation (OGDC), release 5 (Ma and others, 2009)

In order to construct the database of assets, we followed similar process. We first compiled existing data and/or constructed new data or redelineated existing data where needed. We compiled and reviewed:

- Clackamas County GIS data sets
- Metro Regional Land Information Systems (RLIS) data set
- U.S. Census GIS data set
- Oregon Department of Geology and Mineral Industries (DOGAMI) GIS data sets

See Plate 1 for more details on asset data set sources.

5.0 METHODS

In order to study and evaluate landslide hazard and risk, we performed three primary tasks. First we created detailed data sets of the communities' assets. Next we created detailed landslide hazard data sets. Overview maps of the assets and landslide hazards are displayed on Plates 1 and 2. Finally, we analyzed the hazards and asset data sets together to evaluate potential risk.

5.1 Assets

Community assets are defined as the human artifacts necessary to support a community. Generally, this includes people, property, infrastructure, and economic resources. In this study, assets were limited to permanent population, land and buildings, critical facilities, and primary infrastructure, as detailed below.

5.1.1 Permanent population

People are undeniably the most important asset of a community. Permanent population figures are needed to accurately estimate losses from disasters; however, it is challenging to map this asset because people tend to migrate on yearly, seasonally, monthly, daily, and hourly basis. To assess and geographically distribute permanent population (residents) within the study area, a dasymetric population grid was created.

In the study area, U.S. Census population data are organized in spatial units called census block-groups. Block-groups are statistical divisions of census tracts and generally contain between 600 and 3,000 people. Blocks can be as small as 125 acres (50 hectares) and are typically bounded by streets, roads or creeks. In urban areas census blocks are small, usually defined by one city block, while in rural areas with fewer roads, blocks are larger and can be bound by other geographic features. Within each block-group the census provides no information on the spatial distribution of population. The census provides only one

population number per block-group. To estimate the size and distribution of permanent population for most of the study area, we used dasymetric mapping results developed by the U.S. Geological Survey (USGS) (Sleeter and Gould, 2007). Dasymetric mapping is a process that allocates population data to residential units. Data sets like land cover and census data are used in the dasymetric process to more precisely map population over an area. We attributed with no data those portions of the study area that had no results provided by the USGS. Figure 5 shows permanent population density as a raster with 30-m grid cells.

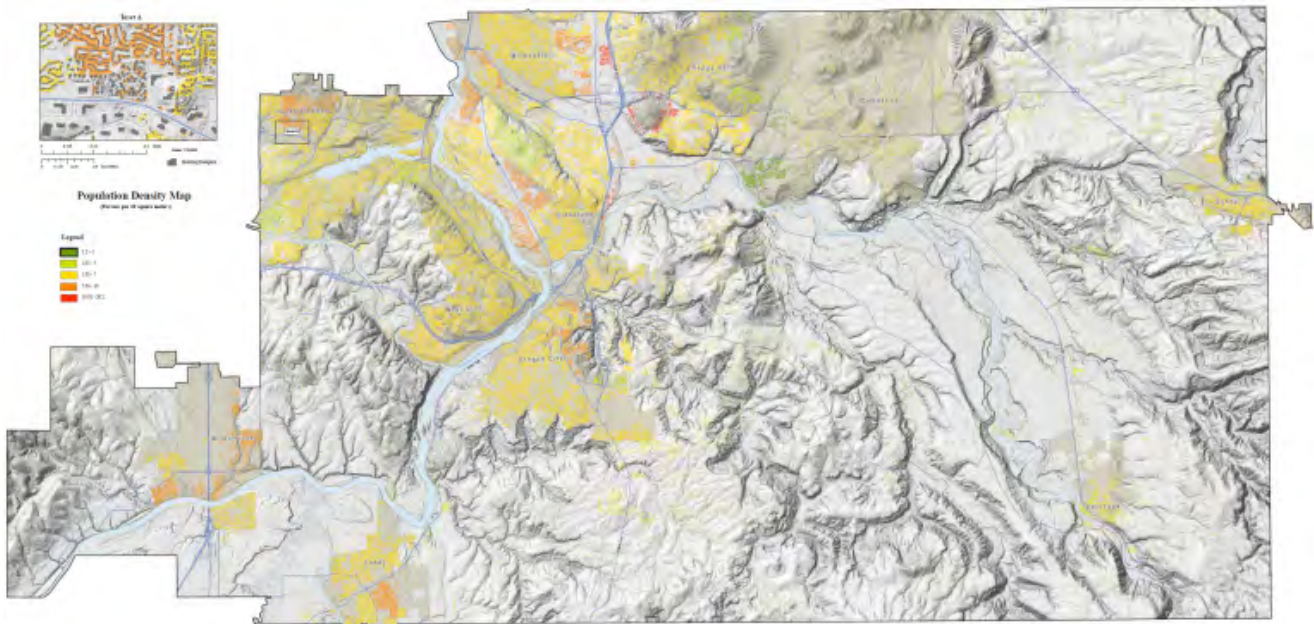


Figure 5. Permanent population in the study area (see Plate 1).

5.1.2 Buildings and land

DOGAMI acquired and edited building locations from Metro's Regional Land Information System (RLIS) (Metro, 2013). Parts of the study area were not covered by the RLIS data, so DOGAMI staff digitized the buildings for those areas. To do this, we converted digital elevation models (DEM derived from lidar first returns) to hillshades and used these in conjunction with orthophotos to locate building locations. After we finalized the generalized land-use layer (see details below), we transferred the improvement values and land-use categories into the building data set (Appendix A).

Zoning refers to the permitted land use designation such as agricultural, industrial, residential, recreational, or other purposes. Zoning data are commonly included in tax lot databases. Data from tax lot databases also include information about the dollar value of the land and any improvements, such as houses. To evaluate land assets for this project, we combined county and city tax lot databases to create a layer that identifies generalized zoning information for each piece of property.

We created the generalized zoning data set with available property tax code data file for Clackamas County acquired from RLIS. Starting with the generalized zoning data set, we then assigned each tax lot a generalized occupancy class used in the FEMA Hazus-MH program. The eight classes are agriculture, commercial, education,

government, industrial, single family, multi-family, and religion (Figure 6). We classified generalized occupancy classes from the parcel's defined chief zoning and land-use of the property. This methodology potentially introduces errors where the tax code for a parcel might not reflect real infrastructure or use at time of publication. We classified selected property that had no ownership information or property tax code according to occupancy class seen in orthophotos. We classified government and education occupancy parcels from existing critical facility data sets. Community (sometimes jurisdictional) boundaries were manually populated, so that parcel counts were not duplicated during inventory/exposure analysis. In scenarios where parcels crossed multiple community boundaries, we selected the boundary to which the parcel appeared to be most appropriately associated. See Appendix A for a detailed breakdown of the zoning, land-use, and occupancy classes.

We clipped the generalized land-use layer to the study area, thereby reducing the original size of some of the parcels along the study area boundary. In order to determine the real market value (RMV) of the clipped parcels, we divided the original parcel area by the new clipped area, resulting in a percent size of the original land. We then multiplied this percent by the original RMV value to obtain a more realistic RMV. The parcel RMV value includes only the land value of each parcel, not the value of any structures on the parcel (Burns and others, 2011).

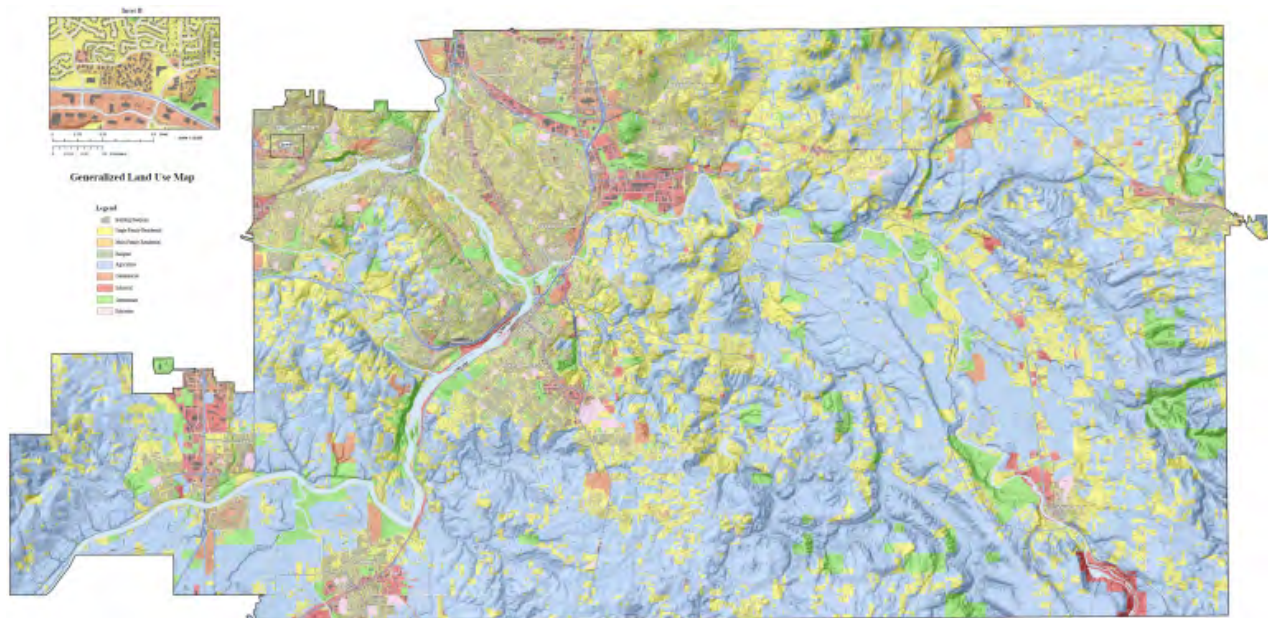


Figure 6. Buildings and land in the study area (see Plate 1).

5.1.3 Critical facilities and primary infrastructure

Critical facilities are typically defined as emergency facilities such as hospitals, fire stations, police stations, and school buildings (FEMA, 2012b). We used the definitions and data created in the DOGAMI Statewide Seismic Needs Assessment (SSNA) (Lewis, 2007) to identify most critical facilities. The critical facilities included in this project are schools, police stations, fire stations, and hospitals (Figure 7). We extracted critical facilities as points from the SSNA. We delineated the land under each critical facility using first-return lidar DEMs, 2009 National Agriculture Imagery Program (NAIP) orthophotos, and available tax lot data. Critical facility land includes any associated buildings, parking lots, leased lands, and land owned by the facility.

Primary infrastructure for this study includes roads, high voltage (approximately 230 kilovolts and greater) electric transmission line towers, substations, power-generating dams, and railroads (Figure 7). We selected this limited set of infrastructure because data were readily available and/or easy to produce from first return lidar or orthophotos. The following list summarizes the data sets:

Transportation (four data sets)

- freeways, highways, and major arterials – lines
- minor arterials and collectors/connectors – lines
- local streets – lines
- railroads – lines

Electric (three data sets)

- transmission line towers – points
- substations – polygons
- power generating dams – polygons

We acquired the road and railroad data from RLIS. We found the railroad data to have significant spatial error when compared to the lidar-based imagery, so DOGAMI staff spatially adjusted railroad lines.

DOGAMI staff digitized electric transmission towers, substations, and power-generating dams in GIS by using the first-return lidar DEMs and 2009 NAIP orthophotos.

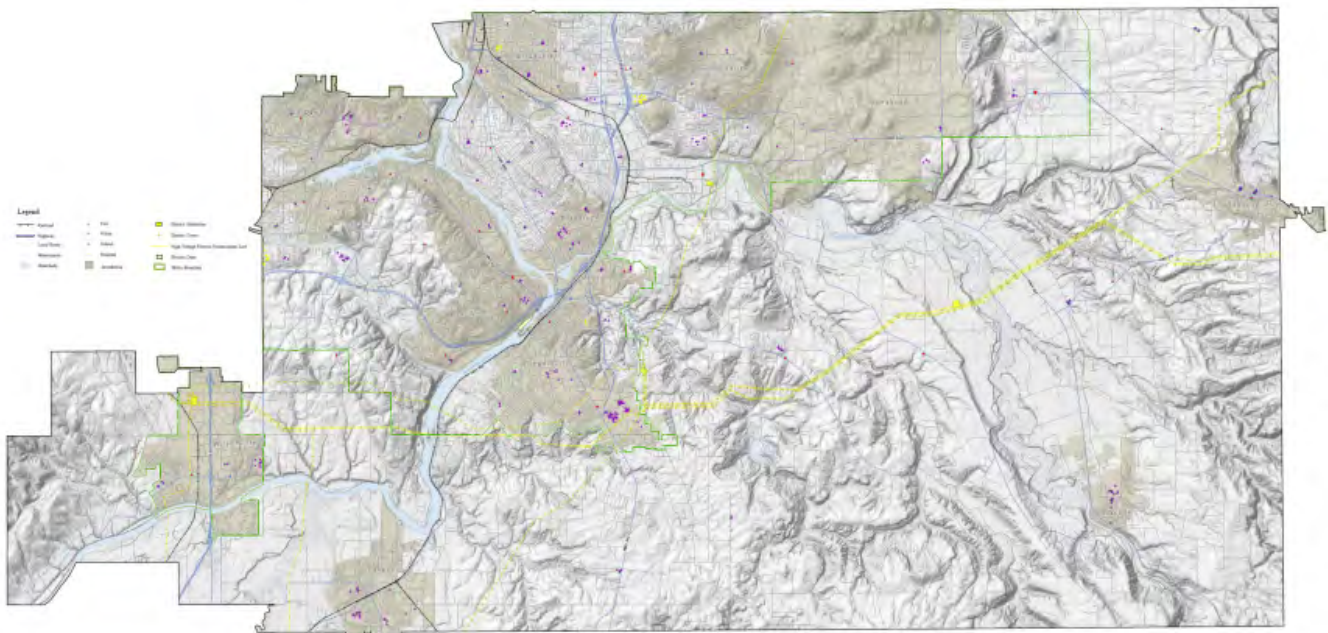


Figure 7. Critical facilities and primary infrastructure in the study area (see Plate 1).

5.2 Landslide hazards

The general term landslide refers to the movement of earth materials down slope. Landslide movement can be classified into six types: falls, topples, slides, spreads, flows, and complex (Turner and Schuster, 1996). Movement type is often combined with other landslide characteristics such as type of material, rate of movement, depth of failure, and water content in order to more fully describe the landslide behavior. Slope areas that have failed remain in a weakened state and are particularly important to identify as these areas may be susceptible to instability (Burns and Madin, 2009; Appendix B). Although water is the most common trigger for landslides, earthquakes can also induce landslides.

Channelized debris flows are one of the most potentially life-threatening types of slide due to their rapid movement down channel and because they can travel several miles down slope. Debris flows tend to initiate in the upper reaches of a drainage and pick up water, sediment, and speed as they come down the channel. As a debris flow

approaches the mouth of a channel, the material tends to fan out due to the lower slope gradient and lack of confinement. Debris flows are commonly mobilized by other types of landslides failing on slopes near the channel or from accelerated erosion during heavy rainfall or snow melt.

Landslides are often classified by their depth of failure as deep or shallow. Shallow landslides are generally defined as failing above the contact between bedrock and the overlying soil. In this study, shallow landslides are defined as having a failure depth less than 15 ft (Burns and Madin, 2009; Appendix B). Deep landslides have failure surfaces that cut into the bedrock and can cover large areas from acres to tens of square miles.

We separate landslide hazards into landslide inventory and landslide susceptibility data sets. In general, the inventory data show locations of existing landslides and the susceptibility data identify areas with relatively low, moderate, or high likelihood of future landslides. For this study we acquired or created landslide inventory and susceptibility data sets as detailed below.

5.2.1 Landslide inventory

Two landslide inventories are included in this project. The first is a compilation of previously released DOGAMI lidar-based 1:8,000-scale mapping following the methodology of Burns and Madin (2009; also see Appendix B): Canby (IMS-29); Oregon City (IMS-30); Lake Oswego (IMS-32); Sandy (IMS-38); Gladstone (IMS-48); Damascus (IMS-49); Sherwood (IMS-50); Redland (IMS-51); Estacada (IMS-52) (Figure 4).

The second landslide inventory is a compilation of historic landslide locations from the following data sets: historic points and landslide deposits (polygons) with historic dates from the Statewide Landslide Information Database (SLIDO, release 2 [Burns and others, 2011]); current Clackamas County and city (Canby, Damascus, Estacada, Gladstone, Happy Valley, Lake Oswego, Oregon City, Sandy, and Wilsonville) hazard mitigation plans; and limited photo analysis to locate landslides that occurred between 2005 and 2009.

5.2.2 Shallow-landslide susceptibility

To create the shallow-landslide susceptibility map, we followed the protocol developed by Burns and others (2012g; also see Appendix C). Following the method results in a map showing three relative shallow-landslide susceptibility hazard classes: low, moderate, and high.

When we examine the material properties and geometry of a slope, this simplified ratio becomes an equation called the factor of safety (FOS) against landsliding. A

FOS greater than 1 is theoretically a stable slope because the shear resistance (or strength) is greater than the shear stress. A FOS less than 1 is theoretically an unstable slope because the stress is greater than the shear strength. A critically stable slope has a FOS equal to 1 (Appendix C).

To calculate the factor of safety, we need geotechnical material properties. Instead of using existing generalized statewide values (Table 2 in Appendix C [Burns and others, 2012]), we created a new table of material properties (Table 1) for each of the primary surficial geologic units in this specific study area.

We estimated the new material properties from geotechnical reports and borings (Appendix D). In many reports, cohesion and phi (angle of internal friction) values were not tested and therefore were not directly available. Therefore, we estimated these values through empirical correlations from other tests such as standard penetration test blow counts following the method described by Das (1994).

After we acquired the values either directly from reports or through correlations for each surficial geologic unit, we averaged each set of values by geologic unit. DOGAMI and City of Portland geotechnical engineers then reviewed these semi-final ranges of values and averaged values in order to decide the final material properties to be used for this study. The final material properties are displayed in Table 1.

We created a new digital surficial geology/material properties map for the study area (Figure 8). This new map is based on the new lidar-based landslide inventory and previously mapped geology by Ma and others (2012). To

Table 1. Geotechnical material properties (modified from Burns and others [2012]).

	Angle of Internal Friction (ϕ), degrees	Cohesion (c)		Unit Weight (Saturated)		Slope Factor of Safety	
		kPa	lb/ft ²	kN/m ³	lb/ft ³	> 1.5	> 1.25
Landslide deposit (deep failure)	28	0	0	19	122	9.5	11.5
Fill	28	0	0	19	122	9.5	11.5
Alluvium (fine grained)	34	100	2,088	19	122	12.5	15.0
Alluvium (coarse grained)	34	0	0	19	122	12.0	14.5
Troutdale Formation (fine grained)	0	33	689	19	122	11.5	14.0
Troutdale Formation (coarse grained)	0	40	835	19	122	15.0	18.0
Missoula Flood Deposits (fine grained)	30	100	2,088	19	122	12.5	15.0
Missoula Flood Deposits (coarse grained)	34	0	0	19	122	12.0	14.5
Loess	30	100	2,088	19	122	12.5	15.0
Boring lava	28	500	10,440	19	122	12.0	14.5
Rhododendron Formation	30	500	10,440	19	122	20.5	25.0
Columbia River Basalt	40	750	15,660	19	122	30.0	36.0

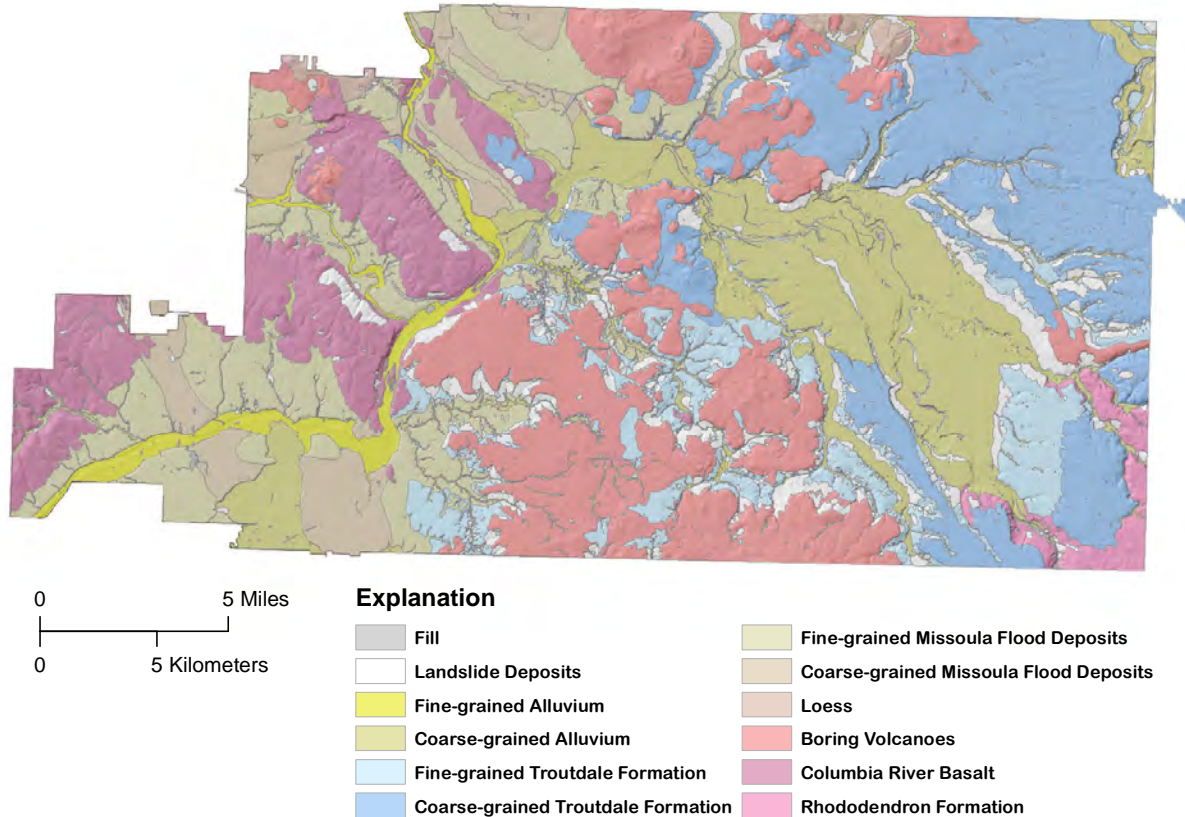


Figure 8. New digital surficial geology/material properties map for the study area.

make the map, we merged and simplified the previously mapped geologic units into 12 surficial geology/material properties units, except for landslide deposits taken directly from the landslide inventory.

5.2.3 Deep-landslide susceptibility

Deep landslides tend to be larger than shallow landslides and tend to move relatively slowly (sometimes less than an inch per year) but can lurch forward if shaken by an earthquake or if disturbed by removing material from the toe, by adding material to the head scarp, or by the addition of water into the slide mass. Reactivation often is focused upslope near the landslide head scarp and at the landslide toe (Turner and Schuster, 1996). To determine deep-landslide susceptibility in the study area, we followed and built on the method described by Burns (2008).

The method we used to identify areas susceptible to deep landslides combines several factors, many of which are derived from the deep landslides extracted from the

SP-42 inventory (Burns and Madin, 2009). We assign each factor a relative score and then combine them into a final data set, which we use to assign areas to low, moderate, or high susceptibility zones. The contributing factors are:

- High susceptibility zone
 - landslide deposits
 - head scarp–flank polygons
 - head scarp–flank polygons buffers
- Moderate susceptibility zone
 - susceptible geologic units
 - susceptible geologic contacts
 - susceptible slope angles for each engineering geology unit polygon
 - susceptible direction of movement for each engineering geology unit polygon
 - minimal landslide deposits and head scarp–flank polygon buffers
- Low susceptibility zone
 - areas not identified in the high or moderate

We created a standardized, blank Esri ArcGIS version 10.1 geodatabase called *Deep_Landslide_Susceptibility_Clackamas_10_1.gdb* to store working and final data. The geodatabase had the following working feature data sets, which can be thought of as subdatabases of the geodatabase:

- A_Landslide_Inventory
- B_Head_Scarp_Flank
- C_Geologic_Units
- D_Geologic_Contacts
- E_Slopes
- F_Direction

To explain the components of the method, we will use throughout this text images of the northwestern quarter of the U.S. Geological Survey Oregon City 7.5-minute quadrangle (Figure 9; Plate 52) The GIS method details are included in Appendix E.

5.2.3.1 High-susceptibility zone

In order to create the high-susceptibility zones, we needed a complete landslide inventory. We created this inventory by using the DOGAMI protocol (Burns and Madin, 2009). An example DOGAMI landslide inventory map made using this protocol is shown in Figure 9 (left).

We first queried all of the deep landslide deposit polygons from the inventory database and saved the data into the A_Landslide_Inventory feature data set in the *Deep_Landslide_Susceptibility.gdb*. We then converted this data set to a raster data set named *High_Deposits* and saved it in the same geodatabase. A portion of the raster data set is shown in Figure 9 (right).

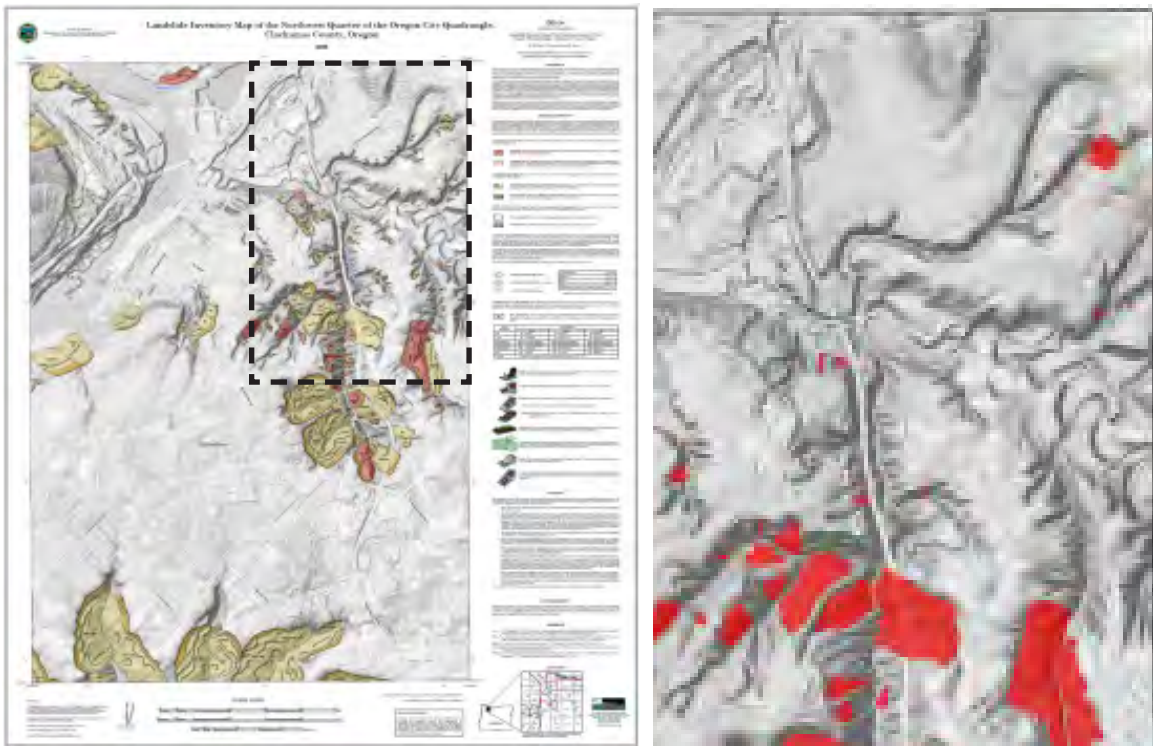


Figure 9. (left) Example of a lidar-based landslide inventory map (Burns and Mickelson, 2010). Dashed line indicates extent shown in figure on the right. (right) Example of deep landslide deposits converted to high-susceptibility zone (red areas on map) (Burns and Mickelson, 2010).

5.2.3.2 Head scarp–flank polygons and buffers

We queried out all deep head scarp–flank polygons from the inventory database and saved the data into the B_Head_Scarp_Flank feature data set in the Deep Landslide Susceptibility.gdb. We then considered these head scarp–flank polygons to be areas of high susceptibility and included them as part of the head scarp–flank polygon buffers, discussed next. Because the head scarp–flank areas are included in the buffer file, we did not process them individually.

There are many unknowns due to the lack of spatial geological data and spatial data with depth values involved in regional deep landslide susceptibility mapping, so to account for some of these unknowns we applied two buffers to the high-susceptibility zone: 1) 2H:1V buffer on all head scarp–flanks and 2) head scarp–flank retrogression buffer.

We applied these buffers to all deep head scarp–flank polygons from the landslide inventory. In most cases the head scarp–flank polygon buffer results in a minimal buffer distance, and the head scarp retrogression buffer results in the maximal buffer distance. In all cases we used the greater of the two distances as the buffer value.

5.2.3.2.1 Head scarp–flank polygon 2H:1V buffer

Most landslides tend to leave a near-vertical head scarp above the failed mass (Turner and Schuster, 1996). Commonly, this head scarp area fails retrogressively or a separate landslide forms above the head scarp, because of the loss of resisting forces. Generally, the area above the head scarp has a relatively low slope angle, possibly indicating a low susceptibility to future failure. In many cases, however, the opposite is true; that is, the flat area directly above the head scarp (crown) is highly susceptible to failure. In order to account for the increase in susceptibility of this area above the head scarp, which may be missed by using the slope alone or in case a particular deep landslide has no internal down-dropped blocks, we apply a 2H:1V head scarp buffer (Figure 10). This buffer is different for each head scarp and is dependent on head scarp height. For example, a head scarp height of 16.5 ft has a 2H:1V buffer equal to 33 ft.

The 2 horizontal to 1 vertical ratio (2H:1V) is commonly used in geotechnical engineering because the slope angle of a 2H:1V slope is equal to 26° (Figure 11) (Burns and others, 2013). This is important because most natural, intact (non-landslide) geologic units have an angle of internal friction or equivalent shear strength of at least 26° .

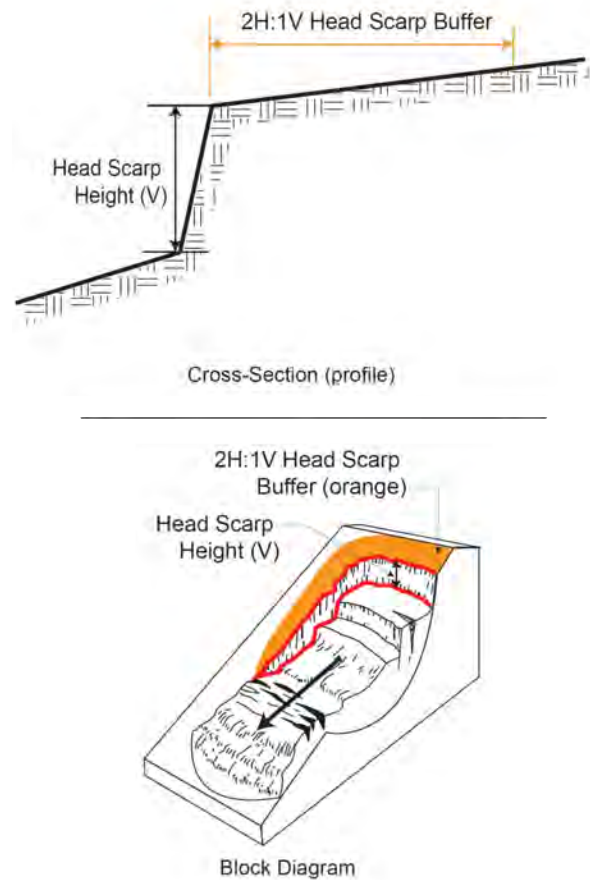


Figure 10. Diagram of the 2 horizontal to 1 vertical (2H:1V) head scarp buffer (orange on block diagram).

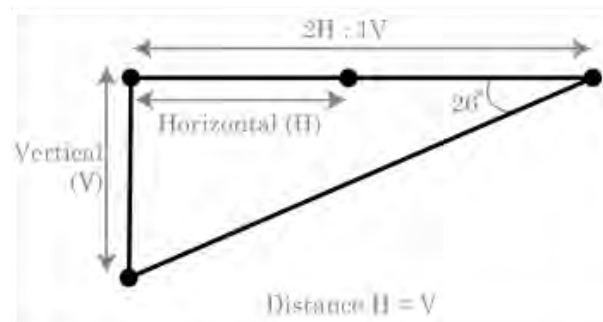


Figure 11. Diagram of the 2 horizontal to 1 vertical (2H:1V) ratio.

5.2.3.2.2 Head scarp–flank polygon retrogression buffer

Many deep landslides move repeatedly over hundreds or thousands of years, and many times the continued movement is through retrogressive failure (continued upslope failure) of the head scarp into the crown. In order to account for this potential upslope hazard, we applied a buffer to all the head scarp–flank polygons as shown in Figure 12. In order to calculate the head scarp retrogression buffer, we measure the horizontal distance of each of the internal down-dropped blocks (assumed to be previous retrogression failures) and use the average. The second buffer is also different for each head scarp and is dependent on the average of the horizontal distance between internal scarps.

After we created both buffers, we combined them and then converted them to a raster data set named High2 (see Appendix E) saved in the Deep Landslide Susceptibility.gdb. The finished data set is shown in Figure 13.

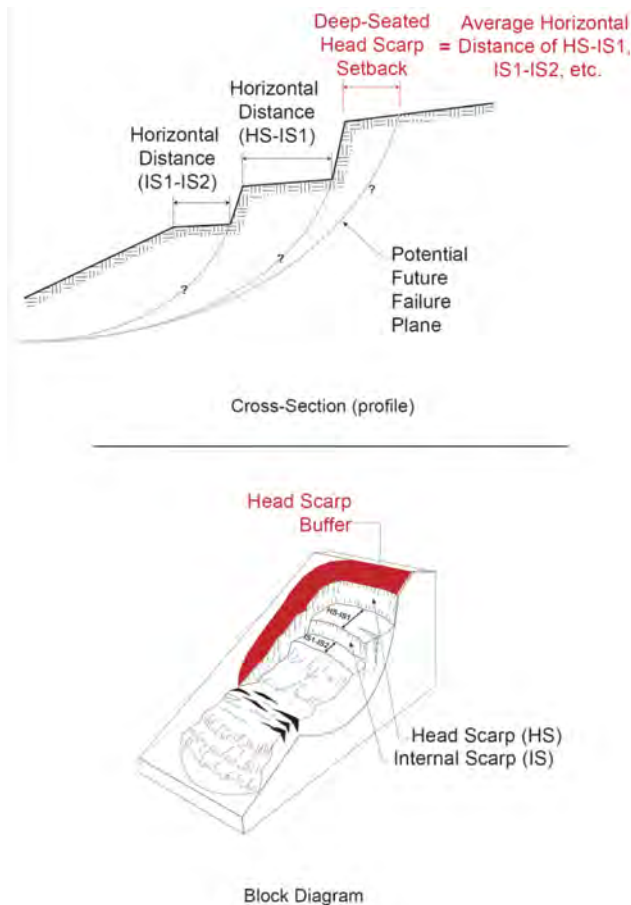


Figure 12. Head scarp retrogression buffer.

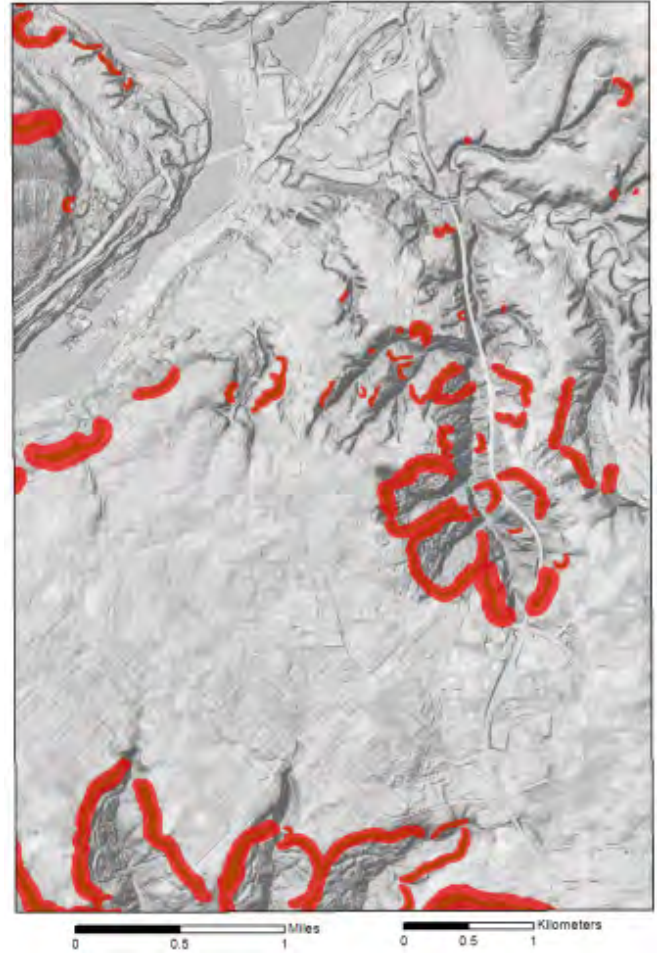


Figure 13. Example of the buffered deep-landslide head scarp–flank polygons converted to high-susceptibility zone (red areas on map). Brown areas are the mapped head scarp–flank polygons.

5.2.3.3 Moderate susceptibility zone

We created the moderate susceptibility zone by combining four maps made from four susceptibility factors described below and a minimal buffer around landslide deposits and head scarp–flank polygons. We used the four susceptibility factors and buffer to determine the boundary between the moderate and low susceptibility zones. (The high-susceptibility zone was defined in section 5.2.3.1.) The four factors are:

- susceptible geologic units
- susceptible geologic contacts
- susceptible slope angles for each engineering geology unit polygon
- susceptible direction of movement for each engineering geology unit polygon

These factors have been used or recommended by others to predict future landslide locations and/or susceptibility (Wilson and Keefer, 1985; Giraud and Shaw, 2007; Baum and others, 2008; Soeters and van Westen, 1996; Sidle and Ochiai, 2006; Schulz, 2007). We selected each of these factors for reasons explained below.

The first factor, geologic unit, has a relatively widespread correlation with surficial processes. For example, it is very common that certain geologic formations or units are more or less prone to landslides. This is generally due to the properties of the unit, such as material strength or planes of weakness within the unit.

The second factor, geologic contacts, we found to be significant in Oregon, especially after we started mapping landslide inventories using lidar. Many landslides occur along a contact, especially when a sedimentary unit is overlain by an igneous unit. For example, large, deep landslides are located next to each other along the contact between the Troutdale Formation and the Boring Lava (a sedimentary unit below an igneous unit) in the study area (Figure 14). Although it commonly appears that landslide failure occurs at the surface trace (that is, at the contact of the two units in plan view), the failure actually occurs entirely within the Troutdale Formation rather than along the plane between the two units. Very likely, in the distant past, the overlying Boring Lava covered and protected the Troutdale Formation. With time, streams eroded through the Boring Lava and into the Troutdale, exposing the Troutdale and creating low places in the topography (stream canyons) for Troutdale material to slide into. As Troutdale material formed landslides, in some places overlying Boring Lava material was dragged down slope along with the underlying Troutdale.

The third factor, slope angle, is commonly correlated with landslide susceptibility. Most landslide susceptibility maps use slope as the primary or as at least one of the factors to predict future landslide locations. For example, shallow landslides are commonly directly associated with steeper slopes. Deep landslides appear to have less of a direct correlation with slope steepness, which is one reason we included the other three factors (geologic unit, geologic contact, and direction of movement).

The fourth factor, direction of movement, is probably the least commonly used, likely because it is rarely recorded in landslide inventories. We record it at every landslide in our landslide inventory and therefore have data. A standard factor to examine during site-specific evaluations is the local bedding dip and dip direction, because deep

landslides tend to fail along bedding planes or other planes of weakness and in the direction of the dip of those planes. Because we do not have extensive dip and dip direction measurements, we decided to use the recorded direction of movement from the landslide inventory database as a proxy for dip direction or what we are calling preferred landslide direction of movement.

In order to create these four factor data sets, a geologic map is needed. We started with the best available geologic map, and then combine the units into engineering geologic units or units with similar engineering properties. We added a new field and assigned the new engineering geologic unit names, for example “Coarse Terrace Deposits” and saved result into the C_Geologic_Units feature data set in the Deep_Landslide_Susceptibility_Clackamas_10_1.gdb. The Oregon City portion of the final engineering geologic data set is shown in Figure 14.

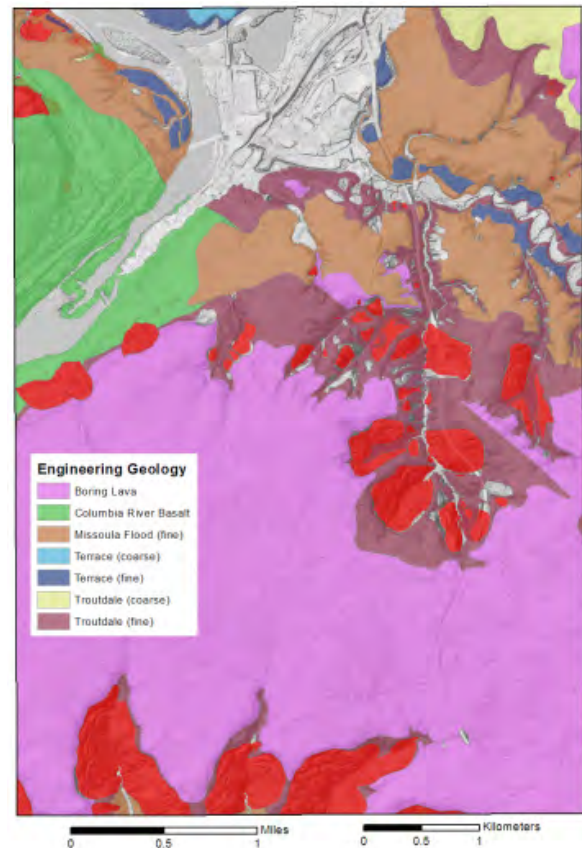


Figure 14. Engineering geology map of the Oregon City portion of the study area.

5.2.3.3.1 Susceptible geologic units

Next, we joined the landslide inventory to the engineering geology. We achieved this spatial join by matching the landslide location with the closest engineering geology unit polygon and matching each landslide one to one with a geologic polygon (see Appendix E). Then we calculated the number of landslides that joined to each engineering geologic unit (Figure 15).

We then used the frequency data to calculate the mean and standard deviation for each unit (Figure 16). We assigned a score of 0, 1, or 2 to each unit:

- score = 0, if less than the mean
- score = 1, if less than mean plus 1 standard deviation and greater than the mean
- score = 2, if equal or greater than mean plus 1 standard deviation

The Oregon City portion of the final map is displayed to Figure 17.

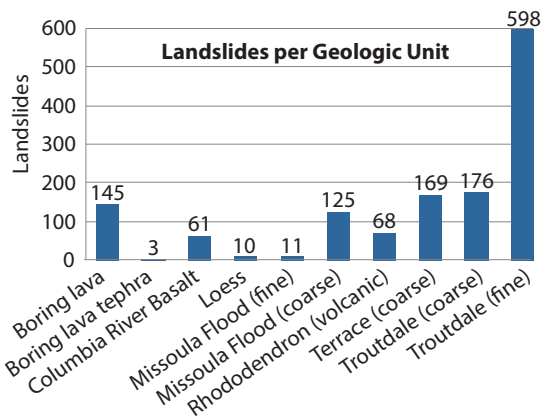


Figure 15. Landslides in each geologic unit in the study area.

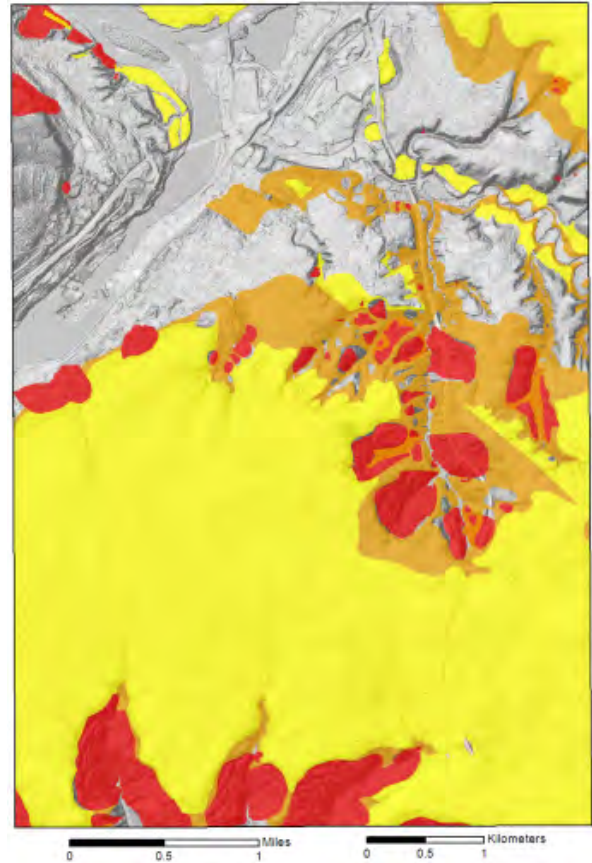


Figure 17. Map of susceptible geologic units factor with scores of zero (no color, gray), one (yellow), and two (orange). Red areas are landslide deposits.

Raw Statistics		Score Derived from Raw Statistics		Score Applied to Engineering Geology Unit		
Mean	137	Mean + 1 STD	312 equal or greater	2	Frequency	145
Standard Error	55	Mean + 1 STD	312 or less	1	Engineering Geology	Boring lava
Median	97	Mean	137 equal or greater	1	Score	1
Mode	N/A	Mean	137 or less	0		3
Standard Deviation (STD)	175					61
Sample Variance	30,641					10
Kurtosis	6					11
Skewness	2					125
Range	595					68
Minimum	3					169
Maximum	598					176
Sum	1,366					598
Count	10					

Figure 16. Frequency data summary statistics.

5.2.3.3.2 Susceptible geologic contacts

The first step was to identify geologic contacts in the study area that have landslides along them (Figure 14). We selected the units on each side of the contact used the overlapping area of the two polygons to create a new susceptible contact line. We then used this contact line to select landslides that touch or are near the contact (Figure 18). We saved the selected landslides to the D_Geologic_Contacts feature data set in the Deep_Landslide_Susceptibility_Clackamas_10_1.gdb.

After the landslides are selected and saved to a separate file, we executed the minimum bounding geometry (MBG) tool in the Esri ArcGIS™ version 10.1 3D Analyst™ or Spatial Analyst™ extension on the selected landslide file. One of the calculated outputs of this tool is the landslide (MBG) rectangle width, which is normally the length of the landslide from the head to the toe. The mean and standard deviation of the MBG width can be easily calculated for each set of landslides correlated to a particular contact (Figure 19).

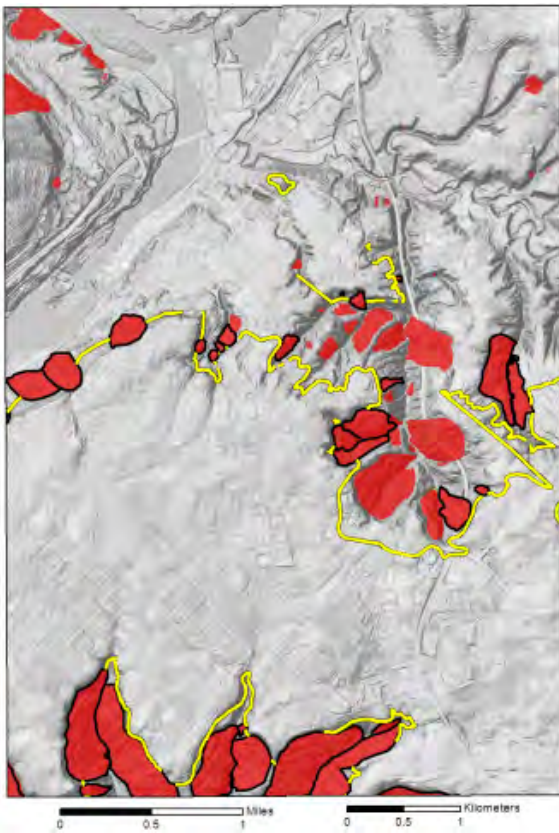


Figure 18. Map of the contact between Boring Lava and fine-grained Troutdale Formation (yellow line) showing landslide deposits (red) and the landslides that touch and are along the contact (red and outlined in black).

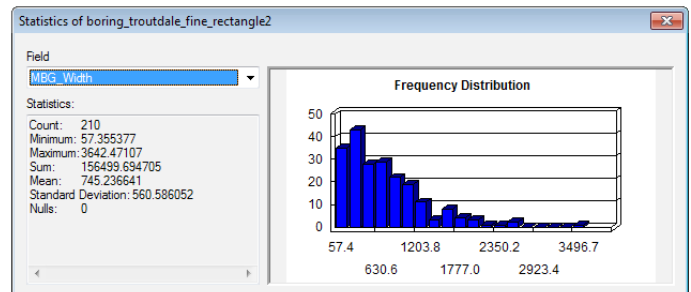
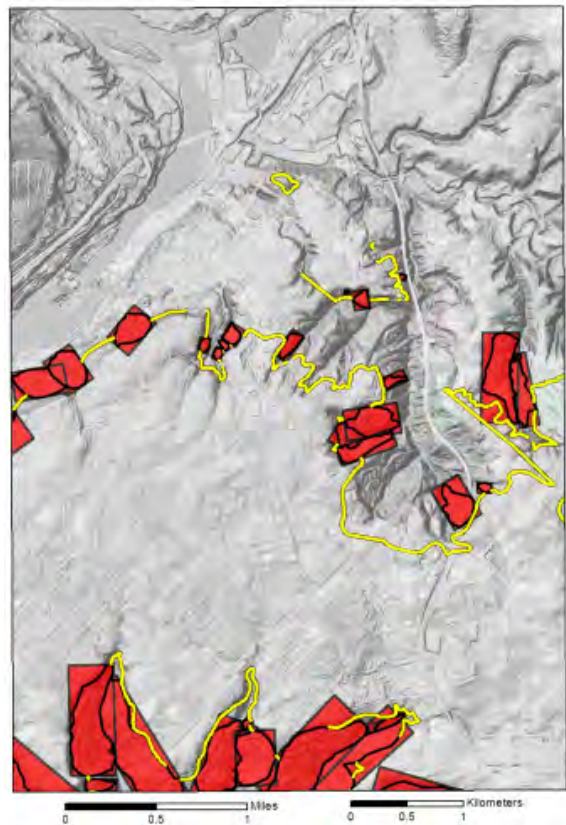


Figure 19. (top) Map of the minimum bounding geometry (MBG) rectangles (black outline and red fill) derived from landslide polygons (black outline inside rectangles). (bottom) Summary statistics of the minimum bounding geometry (MBG) width of landslides with along the contact between Boring Lava and Troutdale Formation.

We then used the mean MBG width distance to create a buffer around the contact line. We assigned this new buffer polygon a score of 2. We used the mean + 1 standard deviation MBG width distance to create a second buffer and we assigned this new polygon a score of 1 (Figure 20).

We repeated this same process for all susceptible contacts and then merged the results into a final susceptible contact factor score file.

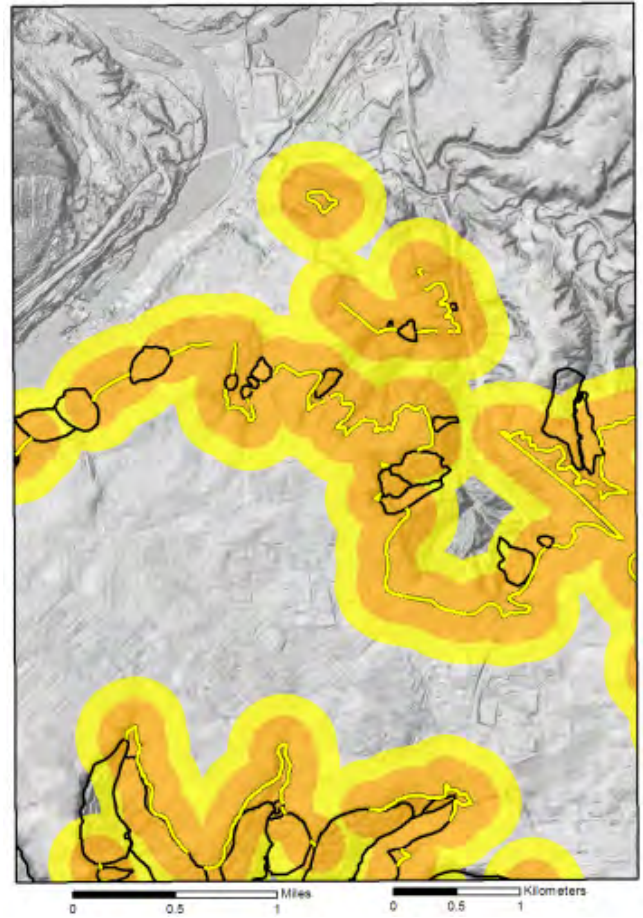


Figure 20. Map of the susceptible contact factor with scores of zero (no color, gray), one (yellow), and two (orange). The contact between the Boring Lava and fine-grained Troutdale Formation is the yellow line, and landslide deposits are outlined in black.

5.2.3.3 Susceptible slopes

Slope angles commonly correlate with landslide susceptibility. In the landslide inventory, the pre-failure slope angle is estimated at each landslide. We used these data to establish slope angle thresholds that have greater potential for future landslides within each engineering geology polygon. We started with the file of joined landslides and engineering geology from section 5.2.3.3.1 (Susceptible Geologic Units). Next we ran the summary statistics tool in ArcGIS and calculated the mean and standard deviation of each susceptible engineering geologic unit. We then joined this table back to the engineering geology file and converted the engineering geology table to a raster of mean slope (Figure 21) and a raster of mean slope plus two standard deviations.

We used the Esri ArcGIS raster calculator to evaluate where on the map the following situations occurred and to assign the following scores:

- score = 2, if slope greater than or equal to landslide mean slope
- score = 1, if slope greater than landslide mean slope and slope greater than mean minus 2 standard deviations slope

The two rasters were added together so that a final susceptible slope factor map is created (Figure 22).

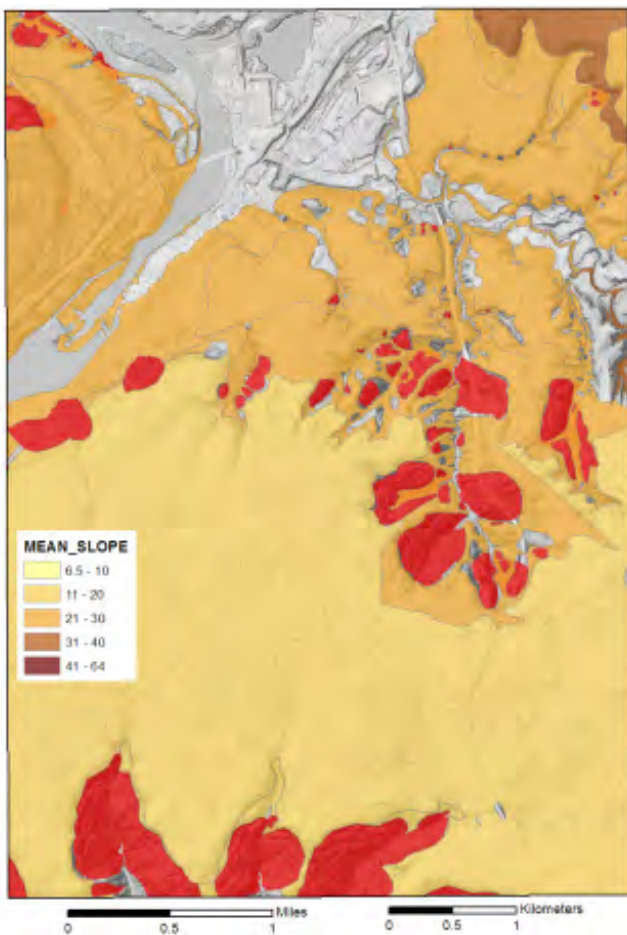


Figure 21. Map of the mean slope angle of each engineering geology polygon derived from landslides (red) located within each polygon.

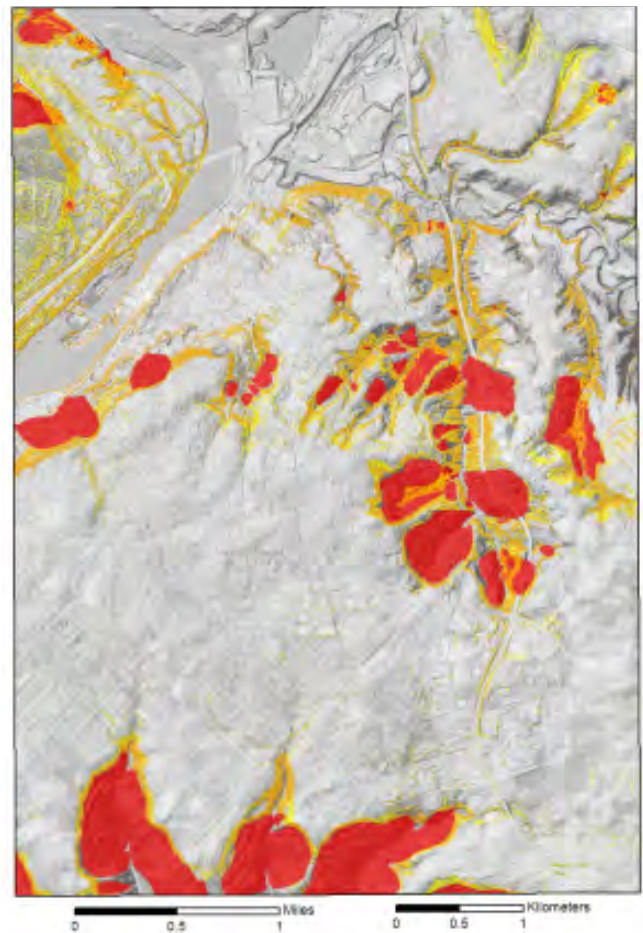


Figure 22. Map of the susceptible slopes factor with scores of zero (no color, gray), one (yellow), and two (orange). Landslides are shown in red.

5.2.3.3.4 Preferred direction of movement

Many deep landslides are partially controlled by subsurface geologic structure. However, structure is rarely factored into modeling due to the lack of detailed spatial understanding of the structure. We recorded the direction of movement at every landslide in our landslide inventory and recommend using these data as a proxy for the geologic structure or preferred direction of movement.

We first converted each landslide area to a grid of points with the direction attribute at each point. Next, we used the file described in section 5.2.3.3.2 (Susceptible Geologic Contacts) with the MBG width to establish the mean width for all landslides within the study area. Then, we interpolated a raster surface from these points using an inverse distance weighted (IDW) technique with a maxi-

imum distance set to the MBG width mean. Finally, we created a slope aspect file from the lidar DEM (Figure 23).

We then used the raster calculator to evaluate where on the map the following situations occur and assign the following scores (see Appendix E):

- score = 2, if [slope aspect less than or equal to (IDW direction of movement plus 22.5)] and [slope aspect greater than or equal to (IDW direction of movement minus 22.5)]
- score = 1, if [slope aspect less than or equal to (IDW direction of movement plus 45)] and [slope aspect greater than or equal to (IDW direction of movement minus 45)]

Because the slope aspect map is very detailed due to the lidar DEM and the map of interpolated landslide direction is very simplified (Figure 23), we decided to use a range

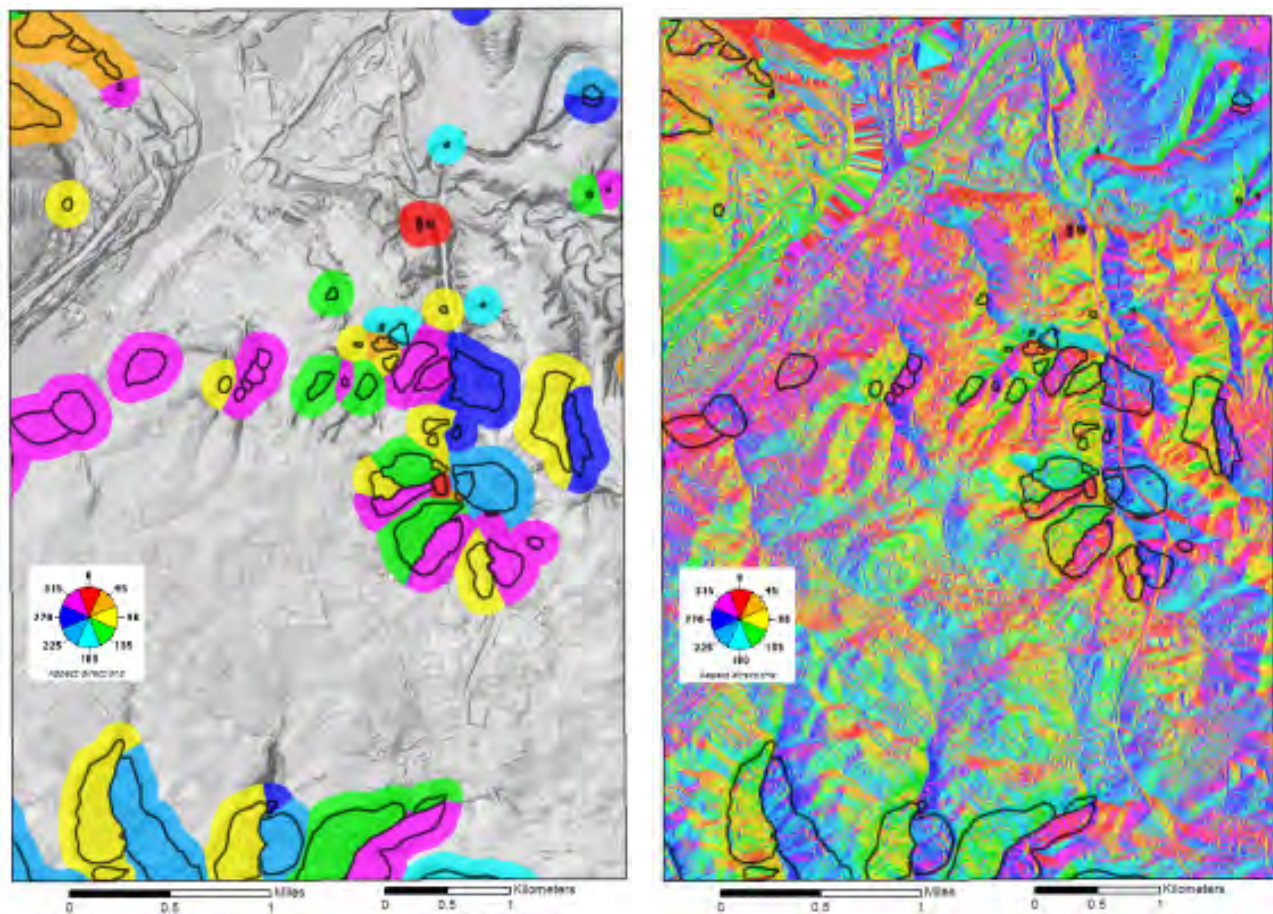


Figure 23. (left) Map of the interpolated landslide direction of movement. (right) Map of slope aspect derived from the lidar DEM. Landslides are outlined in black.

of slope direction. In the case of the higher score (2), any slope within ± 22.5 degrees (45 degrees total) of the interpolated slope is identified. Twice this amount, or ± 45 degrees (90 degrees total), is used for the medium score (1). We then added the two rasters together to create a final susceptible preferred direction factor map (Figure 24).

5.2.3.4 Combined moderate factors score

We then combined the four factor maps (geologic units, geologic contacts, slope angles, and direction of movement). Each factor map is made up of raster cells and each cell has a score of 0, 1, or 2, so the final combined map has a range of values from 0 to 8. A score of zero means none of the factors were present at a particular site, and a score of 8 means the maximum value for all four factors was present (Figure 25).

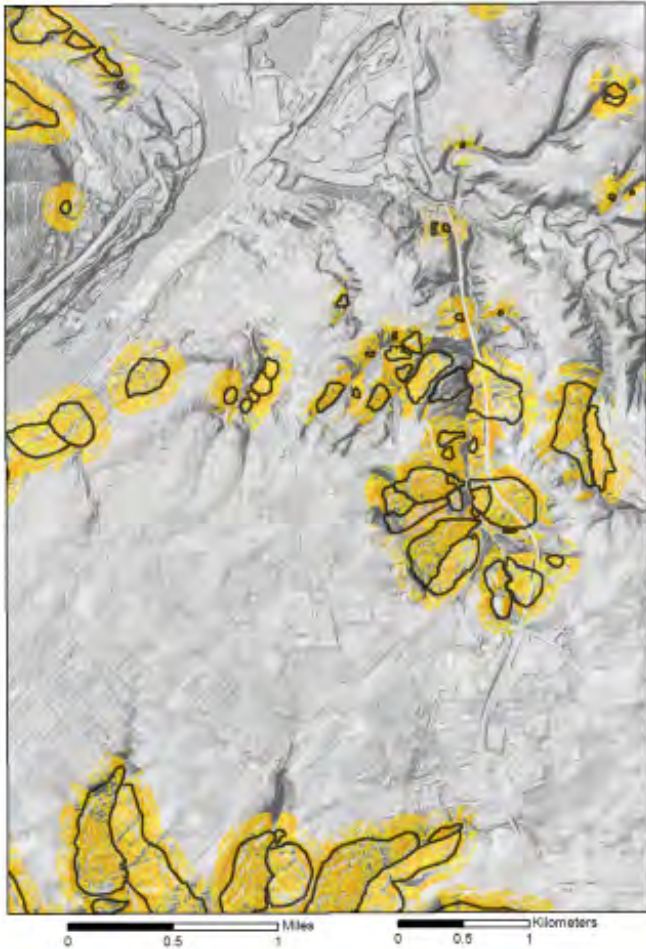


Figure 24. Map of the susceptible preferred direction factor with scores of zero (no color, gray), one (yellow), and two (orange). Landslides are outlined in black.

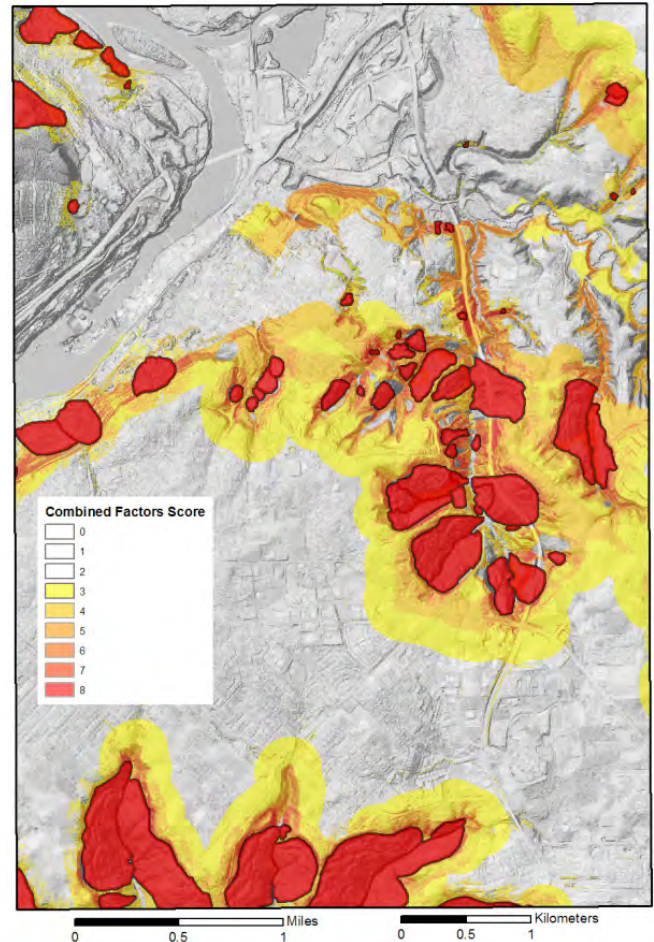


Figure 25. Map of the combined moderate factor scores with total scores ranging from zero (no color, gray) to eight (red). The high-susceptibility zone defined in section 5.2.3.1 is shown in red outlined in black.

5.2.3.5 Minimal landslide deposits and head scarp–flank buffers

To establish a minimal moderate susceptibility zone around the landslide deposits and head scarp–flank polygons, we multiplied the head-scarp height by two, just as we did in section 5.2.3.2 (Head scarp–flank polygons and buffers). This establishes a minimal distance for each landslide on the basis of individual landslide attributes (Figure 26, left).

5.2.3.6 Delineation of the moderate susceptibility zone

We used the minimal moderate susceptibility zone and the combined moderate factors map to delineate the line between the moderate and the low susceptibility zone. We used a minimal combined factor score threshold between 3 and 5 along with educated judgment to delineate the boundary between the low and moderate zones (Figure 26, right).

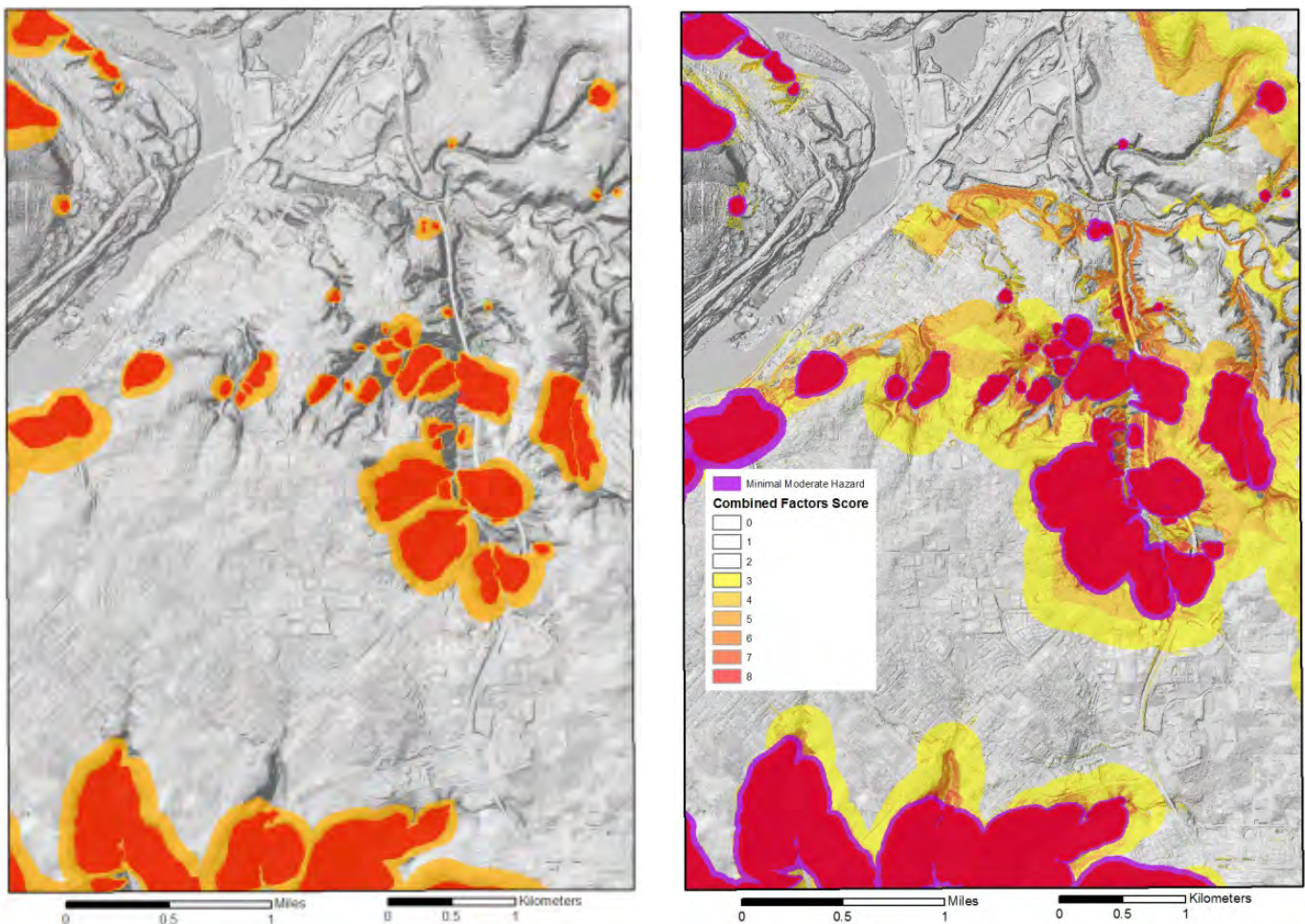


Figure 26. (left) Map of the minimal moderate susceptibility zone (orange) and landslide deposits (red). (right) Map of the high susceptibility zone (red), the combined moderate factors score (yellow to orange areas), and the minimal moderate zone (purple).

An example of educated judgment can be seen in the northwest portion of Figure 267. This area lacks moderate factors and minimal moderate zone; however, a known Columbia River Basalt soil interbed in this area called the Vantage Horizon is exposed at the surface. Just to the west of this area a large landslide, which very likely failed along the Vantage Horizon, occurred.

5.2.3.7 Final deep-landslide susceptibility zones

The final deep landslide susceptibility zones are a combination of contributing factors discussed in the previous section 5.2.3 and combined as shown in Table 2 (Figure 27).

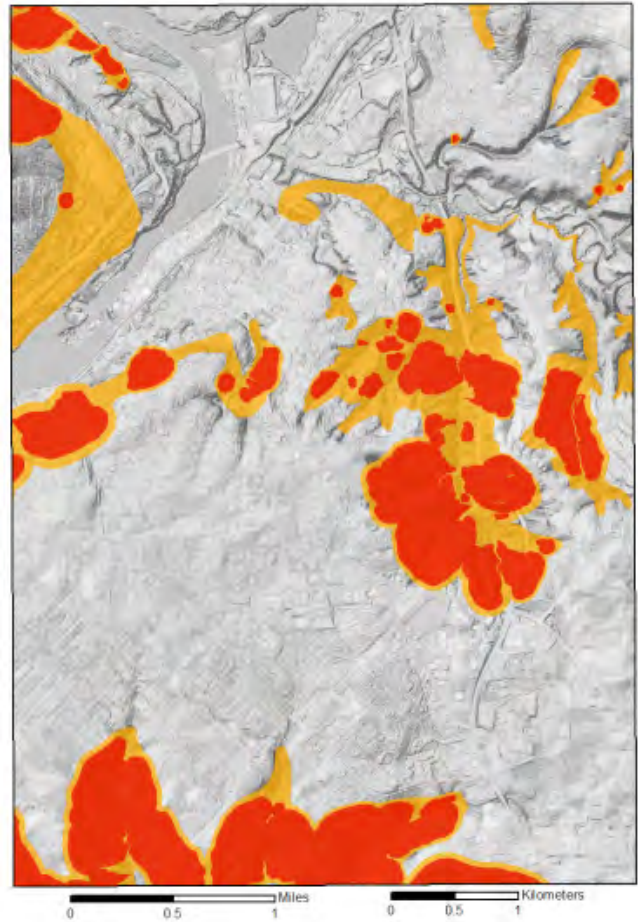


Figure 27. Map of high (red), moderate (orange), and low (no color, gray) deep-landslide susceptibility zones.

Table 2. Final deep-landslide hazard zone matrix.

Contributing Factors	Final Hazard Zone		
	High	Moderate	Low
Landslides, Head Scarp–Flanks, Buffers	included	—	—
Geologic Factors, High Zone Buffer	—	included	—
Minimal Geologic Factors	—	—	included

5.2.3.8 Deep-landslide susceptibility map

We developed a map template as part of the protocol described here. The map template provides a way to display deep-landslide susceptibility data in a consistent manner for any area in Oregon. An example of this template is shown in Figure 28.

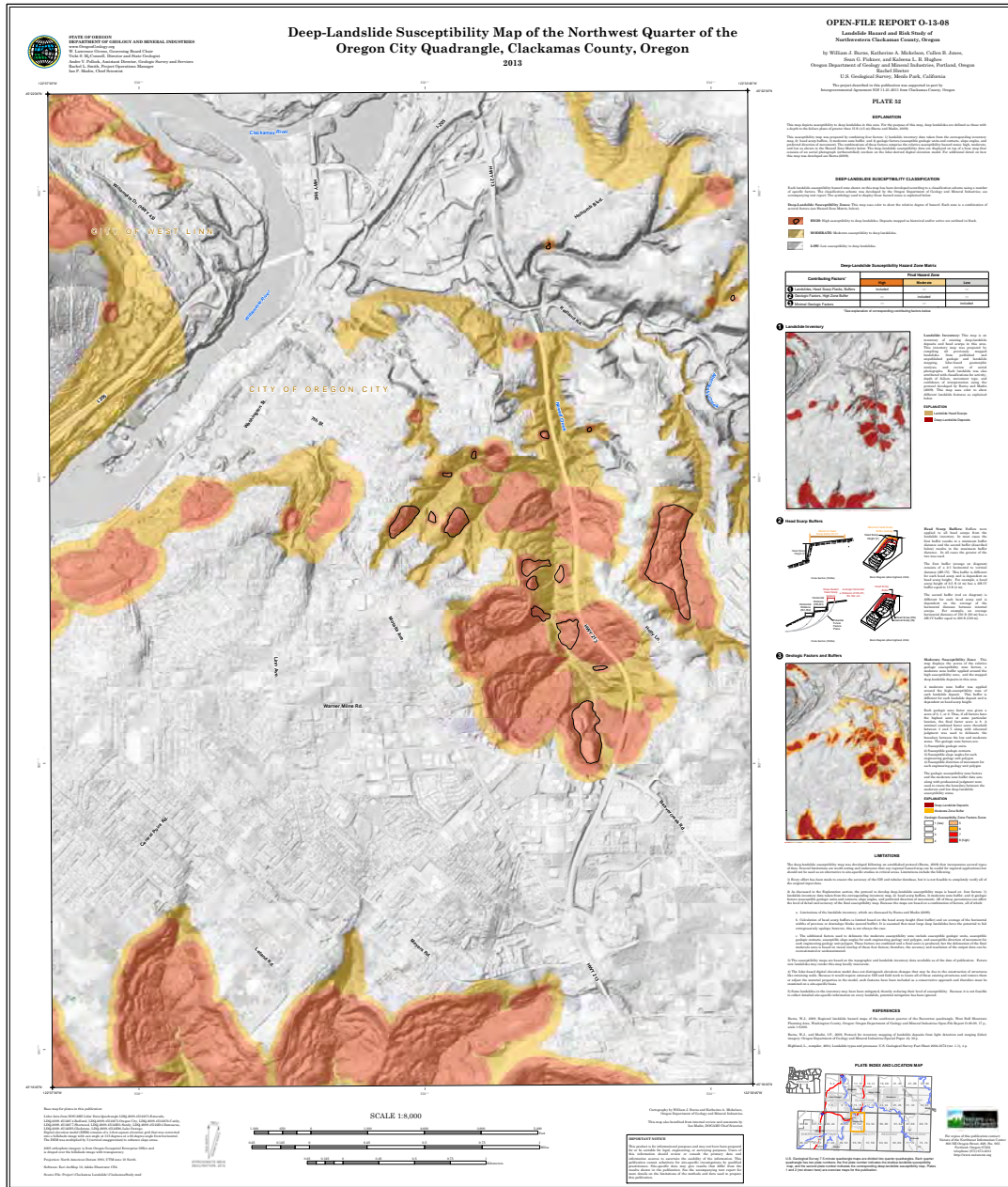


Figure 28. Example of the deep-landslide susceptibility map of the northwest quarter of the U.S. Geological Survey Oregon City 7.5-minute quadrangle, Clackamas County, Oregon (Plate 52).

5.3 Risk Analysis and Loss Estimation

When landslides affect humans, they become natural hazards. Natural hazard risk assessment is the characterization of the overlap of natural hazards and humans (assets).

Risk analysis can range from simple to complicated. In this project we selected two types of regional risk analysis: 1) hazard and asset exposure and 2) Hazus-MH, a multi-hazard analysis program that estimates physical, economic, and social impacts of a disaster (FEMA, 2011). In order to better understand the risk, we also collected historic landslide data for the study area and estimated actual historic losses.

5.3.1 Exposure analysis

Simply put, a building is considered to be exposed to the hazard if it is located within a selected hazard zone. We performed exposure analysis with Esri ArcGIS version 10.1 software. We determined exposure through a series of spatial and tabular queries between hazard zones and assets and reported by the community (spatial extents) as shown in Table 3.

Hazard zones used in the exposure analysis are:

- shallow landslides (inventory)
- deep landslides (inventory)

Table 3. Communities for exposure reporting.

Community	Area		Percent of Study Area
	mi ²	acres	
Metro urban growth boundary area*	136.65	87,456	36.7%
Clackamas County (non-city)	290.92	186,188	78.1%
Canby	4.39	2,811	1.2%
Damascus	16.09	10,295	4.3%
Estacada	2.29	1,465	0.6%
Gladstone	2.49	1,594	0.7%
Happy Valley	9.19	5,881	2.5%
Lake Oswego	11.59	7,415	3.1%
Milwaukie	5.16	3,304	1.4%
Oregon City	9.85	6,305	2.6%
Sandy	3.19	2,042	0.9%
West Linn	8.18	5,238	2.2%
Wilsonville	7.42	4,747	2.0%
Other jurisdictions**	1.60	1,024	0.4%
Total	372.36	238,308	—

*Metro values not included in totals.

**Johnson City, Rivergrove, Barlow, Portland (< 0.5 mi²), and Tualatin (< 0.8 mi²)

- debris flow fans (inventory)
- shallow landslide susceptibility (low)
- shallow landslide susceptibility (moderate)
- shallow landslide susceptibility (high)
- deep landslide susceptibility (low)
- deep landslide susceptibility (moderate)
- deep landslide susceptibility (high)

In other words, we used the GIS databases to find which community assets fell in which hazard zones. For example, we superimposed the buildings layer for the City of Lake Oswego on the deep-landslide high-susceptibility zone layer to determine which buildings are exposed to that level of hazard. The result of this analysis is both a map of the community assets exposed to the hazard and a table with the corresponding numbers of community assets exposed.

Asset data used in the exposure analysis are:

- population (people per 30 m² [323 ft²])
- buildings and land
 - merged into eight generalized occupancy classes (zoning/land use classes) used in FEMA Hazus-MH: single family residential, other residential, commercial, industrial, agriculture, religion, government, education
 - buildings reported by count, count percent of total, and value (dollars)
 - land reported by count, count percent of total, area (square feet), area (acres), area percent of total, value (dollars)
- critical facilities buildings and land
 - hospitals
 - fire stations
 - police stations
 - school buildings
 - buildings reported by count, count percent of total, and value (dollars)
 - land reported by count (parcel county), count percent of total, area (square feet), area (acres), area percent of total, value (dollars)
- transportation
 - freeways, highways and major arterials – lines
 - minor arterials and collectors/connectors – lines
 - local streets – lines
 - railroads – lines
 - report by length (feet), length (miles), and percent of total
- electric
 - major transmission line towers – points, reported by county and percent of total

- major substations – polygons, reported by count
- power generating dams – polygons, reported by count

Some assets were divided into the numbers of miles exposed to the hazard. These assets are generally the primary infrastructure lifelines or linear systems such as roads and rail lines. For the generalized occupancy classes asset layer, we multiplied the portion of the parcel exposed (percent of the total parcel size) by the parcel's total dollar value, so that a realistic exposed land dollar value could be obtained.

To accomplish the task of analyzing 2,093 different asset output values (including totals and per community numbers) for each of the nine hazard zones, we created a GIS model. The model resulted in 18,657 different output values. Details about the model and the exposure analysis process are included in Appendix F.

5.3.2 Hazus-MH analysis

We performed the second type of risk analysis with Hazus-MH, a risk modeling software package developed by FEMA, the National Institute of Building Sciences (NIBS), and other public and private partners (FEMA, 2011). Hazus-MH software can be used to model a variety of earthquake, flood, and wind probabilistic hazards and/or hazard event scenarios. Because there is no landslide module, we used the earthquake module with and without earthquake-induced landslide hazards. Then we subtracted the earthquake-without-landslides model from the earthquake-with-landslides model so that the earthquake-induced landslide damage and losses could be examined separately.

Default databases are included with the Hazus-MH program. Most data are based on national-scale information that generally does not accurately reflect local conditions. To better account for local variability, the software is designed to incorporate user-specific updates to the hazard and asset databases (FEMA, 2011). To update the asset database, much more detailed building-specific data must be collected. Although Hazus-MH has limitations, it is the only publicly available risk analysis program with data for the United States that can produce casualty and fatality estimates. This is one reason why we performed the two types of risk analysis (exposure and Hazus-MH). We also focused on loss ratios rather than absolute numbers, because we know that absolute numbers can be inaccurate at the local scale. For example, instead of examining the

absolute count of buildings at various levels of damage, we looked at the ratio of the estimated damaged buildings to the total buildings in the Hazus-MH database. Although the absolute numbers may be inaccurate, the ratios are very likely in the realistic range and could be applied to the much more accurate local database to obtain a realistic absolute number.

The smallest areal extent allowed for analysis in the Hazus-MH earthquake module is the census tract level. We chose this level for all analyses. We selected the 60 census tracts that best represent the study extent (Figure 29). Although the extent of the 60 tracts is in some places larger than the study area and in some places smaller, overall we felt it best represented the study area. One limitation of Hazus-MH is that census tract areas can be too coarse for small areas mapped as hazard zones.

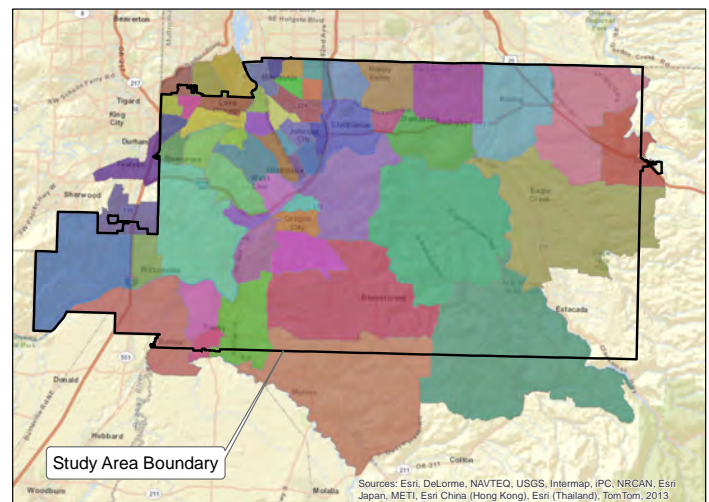


Figure 29. Map of the 60 selected census tracts in the study area used in the Hazus-MH analysis.

The goal was to estimate damage and losses from two kinds earthquakes (crustal and Cascadia Subduction Zone), both with and without earthquake-induced landslides, so that we could examine the damage and losses caused by just the earthquake-induced landslides. We also ran landslides set to 9 out of 10 (Table 4, IX values) for a single scenario to make sure the changes were continuing above the analysis level (detailed landslides). We performed five different Hazus-MH analyses (Table 5; Appendix H).

Table 4. Landslide susceptibility of geologic groups (Hazus-MH 2.0, Table 4-15 [FEMA, 2011]).

Geologic Group	Slope Angle, degrees					
	0–10	10–15	15–20	20–30	30–40	>40
(a) DRY (groundwater below level of sliding)						
A Strongly cemented rocks (crystalline rocks and well-cemented sandstone, $c' = 300$ psf, $\phi' = 35^\circ$)	none	none	I	II	IV	VI
B Weakly cemented rocks (sandy soils and poorly cemented sandstone, $c' = 0$, psf, $\phi' = 35^\circ$)	none	III	IV	V	VI	VII
C Argillaceous rocks (shales, clayey soil, existing landslides, poorly compacted fills, $c' = 0$, psf, $\phi' = 20^\circ$)	V	VI	VII	IX	IX	IX
(b) WET (groundwater level at ground surface)						
A Strongly cemented rocks (crystalline rocks and well-cemented sandstone, $c' = 300$ psf, $\phi' = 35^\circ$)	none	III	VI	VII	VIII	VIII
B Weakly cemented rocks (sandy soils and poorly cemented sandstone, $c' = 0$, psf, $\phi' = 35^\circ$)	V	VIII	IX	IX		X
C Argillaceous rocks (shales, clayey soil, existing landslides, poorly compacted fills, $c' = 0$, psf, $\phi' = 20^\circ$)	VII	IX	X	X	X	X

Table 5. Hazus-MH analyses for this study.

Hazus-MH Analysis	Earthquake Scenario	Earthquake-Induced Landslide Hazard Included?
1		no
2	crustal M6.8—Portland Hills Fault	yes, detailed (includes new susceptibility mapping)
3		yes, hazard set to 9 out of 10 (see Table 4, cells with IX values)
4		no
5	Cascadia M9.0	yes, detailed (includes new susceptibility mapping)

The generalized overall landslide hazard data layer (Figure 30) was created following the Hazus-MH methodology (FEMA, 2011). The method combines slope and geologic group as shown in Table 4 to create landslide susceptibility classes. Inside the study extent we combined the geology (Figure 8), the detailed landslide inventory, and the slope map derived from the lidar data. In the few areas of census tracts that extended outside the study area (Figure 29), we used the existing statewide landslide susceptibility values from Madin and Burns (2013).

5.3.3 Historic landslide data and loss estimation

In order to better understand the risk, we also collected historic landslide data for the study area and estimated actual historic losses; 370 historic landslide locations were compiled into a spreadsheet with the following fields:

- year
- damage and loss description
- slide name
- loss/repair costs (dollars)
- location
- comments

Note that not every landslide entry has data for every field; for example, only 299 had dates and only 76 had dollar values.

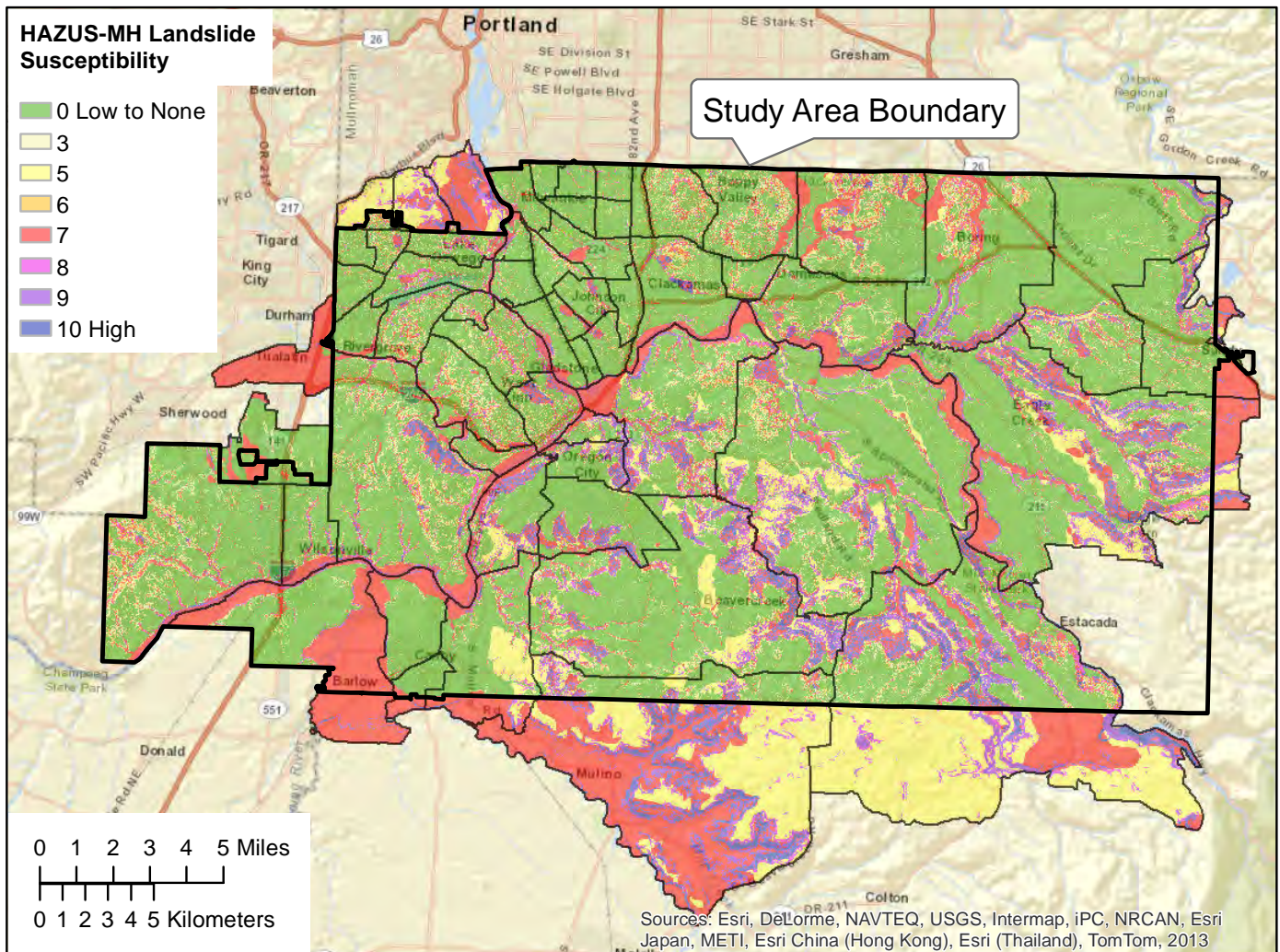


Figure 30. Landslide susceptibility map ranging from 0 (low) to 10 (high) for the Hazus-MH study extent.

6.0 RESULTS

The asset and hazard data sets were all created in ArcGIS and are therefore digital map layers. We acquired, created new, and/or combined published data to create the population, critical facilities and primary infrastructure, buildings and land, landslide inventory, shallow landslide susceptibility, and deep landslide susceptibility data sets.

These data sets are displayed on Plate 1 (asset overview map), Plate 2 (landslide hazards overview map), and Plates 3–74 (detailed susceptibility maps).

6.1 Permanent population results

We created a GIS data set of permanent population for the study area that displays permanent population density gridded at 90 ft (30 m) cell size. There are 339,240 residents in the study area (Table 6), mostly in cities and/or communities (Plate 1); 80% of the population (266,969) falls within the Metro boundary

6.2 Buildings and land results

We created a GIS data set of buildings and generalized occupancy (Figure 6 and Plate 1). There are 153,582 buildings in the study area database with a total real market value of roughly \$22.8 billion. Together, the buildings and land are worth roughly \$40 billion (Table 7, Appendix F).

The generalized land occupancy data set contains eight classes: single family residential, other residential, commercial, industrial, agriculture, religion, government, and education. The data set also identifies individual parcel size, land value in dollars, and improvement (building) value in dollars.

Table 6. Permanent population by community.

Community	Population
Metro urban growth boundary area*	266,969
Clackamas County (non-city)	139,719
Canby	16,334
Damascus	10,354
Estacada	2,794
Gladstone	11,081
Happy Valley	12,910
Lake Oswego	35,736
Milwaukie	21,815
Oregon City	32,506
Sandy	8,645
West Linn	26,132
Wilsonville	16,464
Other jurisdictions**	4,750
Total (Cities + County)	339,240

*Metro values not included in totals.

**Johnson City, Rivergrove, Barlow, Portland (< 0.5 mi²), and Tualatin (< 0.8 mi²)

Table 7. Building and land inventory summary.

Community	Buildings			Land			
	Total Buildings	Percent of Total Buildings	Total Value (dollars)	Parcels	Total Area (acres)	Percent of Total Area	Value (dollars)
Metro urban growth boundary area*	107,229	69.8%	\$18,880,236,254	98156	62473	31.7%	\$12,907,166,251
Clackamas County (non-city)	73,714	48.0%	\$8,206,862,935	50917	164532	80.5%	\$7,555,643,882
Canby	5,601	3.6%	\$775,826,237	5031	2031	1.0%	\$495,837,330
Damascus	6,377	4.2%	\$571,725,843	4379	9516	4.5%	\$497,736,180
Estacada	1,153	0.8%	\$119,127,897	1365	1135	0.5%	\$116,522,395
Gladstone	4,062	2.6%	\$446,203,737	3637	990	0.5%	\$359,239,424
Happy Valley	5,068	3.3%	\$1,097,313,105	6624	4637	2.4%	\$849,768,072
Lake Oswego	13,794	9.0%	\$4,409,759,556	15863	4927	2.6%	\$2,917,432,288
Milwaukie	8,539	5.6%	\$994,967,333	7569	2285	1.1%	\$766,365,219
Oregon City	15,524	10.1%	\$1,728,660,896	11639	4097	2.2%	\$1,037,600,847
Sandy	3,574	2.3%	\$425,193,227	3890	1520	0.8%	\$333,230,683
West Linn	9,273	6.0%	\$1,984,800,222	10311	3073	1.7%	\$1,228,067,655
Wilsonville	5,091	3.3%	\$1,683,958,505	5576	3221	1.8%	\$854,427,273
Other jurisdictions**	1,812	1.2%	\$327,317,776	1510	588	0.4%	\$225,232,317
Total (Cities + County)	153,582	—	\$22,771,717,269	128,310	202,550	—	\$17,236,964,281

*Metro values not included in totals.

**Johnson City, Rivergrove, Barlow, Portland (< 0.5 mi²), and Tualatin (< 0.8 mi²)

6.3 Critical facilities and primary infrastructure results

We created or acquired GIS data to create a data set of critical facilities, defined as hospitals and fire and police and school buildings. We found 424 of these buildings in the study area (Plate 1, Table 8). Most of these buildings were located within the Metro boundary, that is, closer to population centers.

We found roughly 2,300 miles of road and 767 high-voltage electric transmission line towers in the study area (Table 9, Plate 1, Appendix F).

Table 8. Critical facilities inventory summary.

Community	Buildings	Percent of Total Buildings
Metro urban growth boundary area*	340	80.2%
Clackamas County (non-city)	133	31.4%
Canby	21	5.0%
Damascus	4	0.9%
Estacada	16	3.8%
Gladstone	22	5.2%
Happy Valley	12	2.8%
Lake Oswego	32	7.5%
Milwaukie	31	7.3%
Oregon City	82	19.3%
Sandy	16	3.8%
West Linn	22	5.2%
Wilsonville	19	4.5%
Other jurisdictions**	14	3.3%
Total (Cities + County)	424	—

*Metro values not included in totals.

**Johnson City, Rivergrove, Barlow, Portland (< 0.5 mi²), and Tualatin (< 0.8 mi²)

Table 9. Roads and electric system inventory summary.

Community	Road Length		Electric Generating Plants (Dams)	Electric Substations	Electric Towers	
	Total (miles)	Percent of Total			Total	Percent of Total
Metro urban growth boundary area*	1,406	61.0%	2	2	197	25.7%
Clackamas County (non-city)	1,250	54.3%	3	3	640	83.4%
Canby	67	2.9%	0	0	0	0.0%
Damascus	90	3.9%	0	0	0	0.0%
Estacada	23	1.0%	0	0	0	0.0%
Gladstone	46	2.0%	0	0	0	0.0%
Happy Valley	97	4.2%	0	0	25	3.3%
Lake Oswego	182	7.9%	0	0	0	0.0%
Milwaukie	92	4.0%	0	0	0	0.0%
Oregon City	163	7.1%	0	0	34	4.4%
Sandy	46	2.0%	0	0	2	0.3%
West Linn	130	5.6%	1	0	0	0.0%
Wilsonville	94	4.1%	0	1	66	8.6%
Other jurisdictions**	26	1.1%	0	0	0	0.0%
Total (Cities + County)	2,304	—	4	4	767	—

**Metro values not included in totals.

**Johnson City, Rivergrove, Barlow, Portland (< 0.5 mi²), and Tualatin (< 0.8 mi²)

6.4 Landslide inventory results

We created two landslide inventories. The first is a compilation of landslides that were previously mapped by DO-GAMI staff following the methodology of Burns and Madin (2009). We found 2,885 landslides that cover roughly 7% of the study area (Figure 31, Plate 2). Details for each community are shown in Table 10. Of these, 1,367 are large deep landslides and 884 are smaller shallow landslides.

We prepared the following:

- landslide inventory overview map (scale 1:50,000) of the entire study area (Plate 2). Includes an index map to the detailed plates
- landslide inventory geodatabase (Clackamas_landslides_10_1.gdb), which includes 1:8,000-scale landslide inventory data of the entire study area (compiled from IMS-29, -30, -32, -38, -48, -49, -50, -51, and -52)

Table 10. Summary of the northwestern Clackamas County landslide inventory.

Community	Landslides	Area, acres	Percent of Total Area
Metro urban growth boundary area*	654	2,711	3.5%
Clackamas County (non-city)	2,609	15,226	8.2%
Canby	0	0	0.0%
Damascus	58	446	4.3%
Estacada	7	46	3.1%
Gladstone	3	50	3.1%
Happy Valley	20	31	0.5%
Lake Oswego	107	159	2.1%
Milwaukie	4	1	0.0%
Oregon City	62	255	4.0%
Sandy	24	45	2.2%
West Linn	53	265	5.1%
Wilsonville	20	19	0.4%
Other jurisdictions**	2	0	0.0%

*Metro values not included in totals.

**Johnson City, Rivergrove, Barlow, Portland (< 0.5 mi²), and Tualatin (< 0.8 mi²)

Note: Some landslides cross community boundaries and therefore may be counted multiple times; therefore totalling the values in this table will not provide accurate a accurate landslide count, area or percentage.

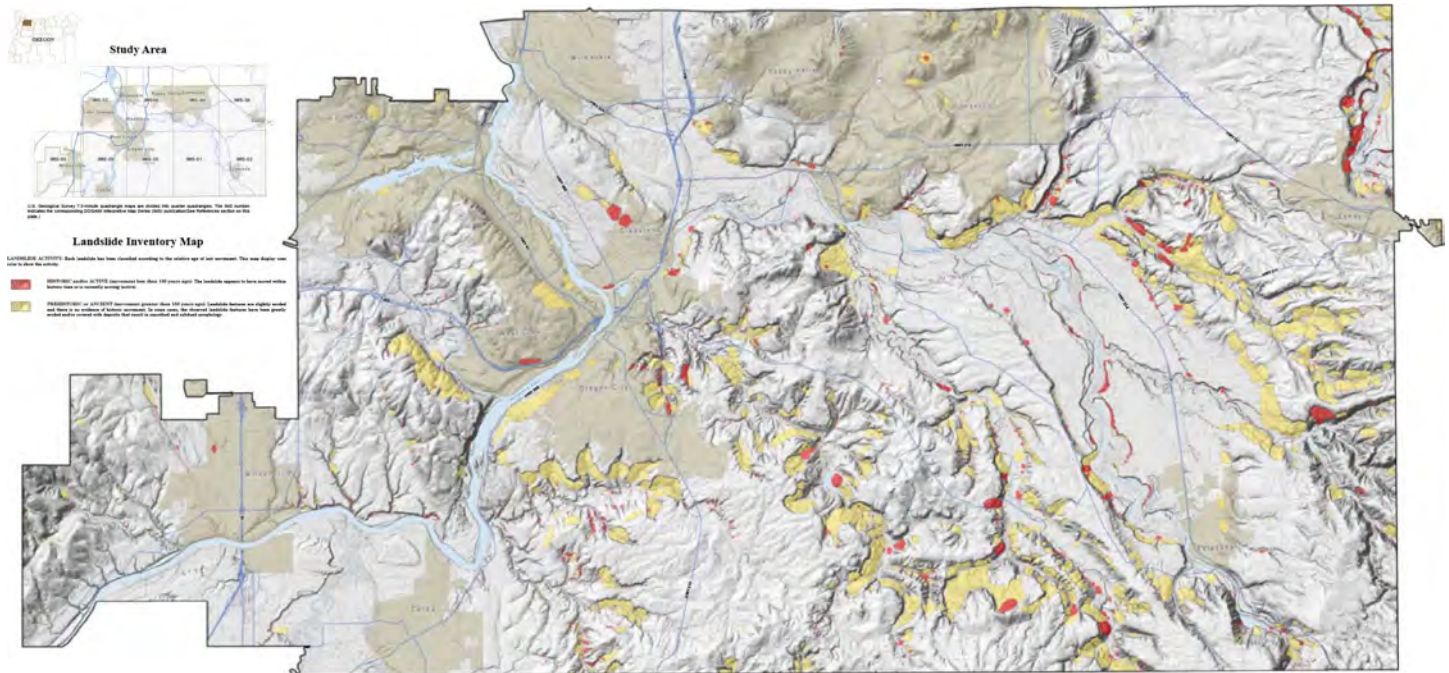


Figure 31. Overview map of the landslide inventory for the study area (see Plate 2).

The second landslide inventory is a compilation of documented historic landslide locations. We compiled 370 landslides that occurred in the study area during the period 1964–2009 (Figure 32; Appendix G). Many of these landslides (200) occurred during the 1996-1997 storm season when three major storms caused thousands of landslides across Oregon (Hofmeister, 2000). However, a significant number of landslides (54) occurred during the period 2006–2009, many (33) during the January 2009 storm (Figure 2).

Many of these historic landslides caused significant damage including homes destroyed as a result of the 1996-1997 landslides and a portion of an apartment complex destroyed in 2005 (Figure 33). Seventy-six of the 370 landslides in this data set had loss or repair costs that added up to \$27.5 million.

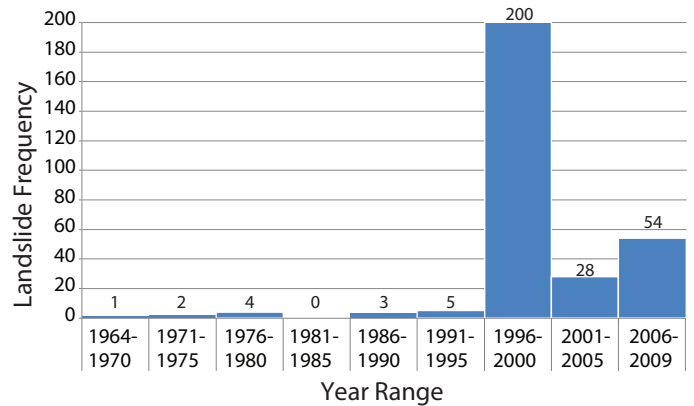


Figure 32. Graph of historic landslides grouped into 5-year bins.



Figure 33. Photographs of historic landslide damage.

(left) Residential home in Oregon City destroyed by a landslide in 1996 (photo from Burns [1998]).

(middle) Apartment complex in Oregon City at the early stages of landslide movement in 2005 (cracks in the foreground); this building was later severely damaged and then demolished.

(right) Landslides along Clackamas River Drive are common almost annually. This one occurred in 2005 and closed the road.

6.5 Shallow-landslide susceptibility results

We found 884 shallow landslides in the study area. The results of the shallow-landslide susceptibility mapping by community varied from 91% low shallow landslide hazard (Canby) to almost 50% combined moderate and high shallow landslide hazard (Happy Valley) (Table 11, Plate 2).

To assist communities in understanding the shallow-landslide susceptibility, we prepared the following:

- shallow-landslide susceptibility overview map (scale 1:50,000) of the study area (Plate 2). Includes an index map to the detailed plates.
- detailed shallow-landslide susceptibility maps (scale 1:8,000) of the study area (36 maps; Plates 3 to 73, odd numbers).
- shallow-landslide susceptibility geodatabase (Shallow_Landslide_Suceptibility_Clackamas_10_1.gdb)

6.6 Deep-landslide susceptibility results

We found 1,367 deep landslides in the study area. These deep landslides were one of the primary factors in the deep-landslide susceptibility mapping. The results of the deep-landslide susceptibility mapping by community varied from 100% low deep landslide hazard (Canby and Milwaukie) to almost 20% combined moderate and high deep-landslide hazard (Clackamas County; non-city) (Table 12, Plate 2).

We prepared the following:

- deep-landslide susceptibility overview map (scale 1:50,000) of the study area (Plate 2). Includes an index map to the detailed plates.
- detailed deep-landslide susceptibility maps (scale 1:8,000) of the study area (36 maps; Plates 4 to 74, even numbers).
- deep-landslide susceptibility geodatabase (Deep_Landslide_Susceptibility_Clackamas_10_1.gdb)

Table 11. Summary of shallow-landslide susceptibility hazard zones by community.

Community	Percent Total Area of Community		
	Low	Moderate	High
Metro urban growth boundary area*	68%	24.7%	7.4%
Clackamas County (non-city)	68%	21.2%	11.0%
Canby	91%	7.5%	2.0%
Damascus	64%	27.7%	8.3%
Estacada	66%	23.9%	10.2%
Gladstone	79%	17.4%	3.7%
Happy Valley	50%	42.9%	6.9%
Lake Oswego	60%	32.1%	7.7%
Milwaukie	75%	21.4%	3.9%
Oregon City	78%	15.2%	7.3%
Sandy	60%	28.9%	10.8%
West Linn	59%	32.7%	8.1%
Wilsonville	79%	16.0%	4.9%
Other jurisdictions**	65%	29.2%	6.0%

*Metro values not included in totals.

**Johnson City, Rivergrove, Barlow, Portland (< 0.5 mi²), and Tualatin (< 0.8 mi²)

Table 12. Summary of deep-landslide susceptibility hazards zones by community.

Community	Percent Total Area of Community		
	Low	Moderate	High
Metro urban growth boundary area*	92.3%	3.6%	4.1%
Clackamas County (non-city)	80.4%	9.2%	10.4%
Canby	100.0%	0.0%	0.0%
Damascus	89.9%	4.4%	5.7%
Estacada	90.0%	6.3%	3.6%
Gladstone	94.8%	1.6%	3.6%
Happy Valley	98.2%	1.2%	0.6%
Lake Oswego	94.5%	3.1%	2.4%
Milwaukie	99.8%	0.1%	0.1%
Oregon City	85.7%	7.9%	6.5%
Sandy	82.8%	8.3%	8.8%
West Linn	86.1%	7.8%	6.2%
Wilsonville	99.8%	0.1%	0.1%
Other jurisdictions**	100.0%	0.0%	0.0%

*Metro values not included in totals.

**Johnson City, Rivergrove, Barlow, Portland (< 0.5 mi²), and Tualatin (< 0.8 mi²)

6.7 Risk analysis and loss estimation results

We performed two types of risk analysis: 1) hazard and asset exposure and 2) Hazus-MH (FEMA, 2005).

6.7.1 Exposure analysis results

We performed hazard and community asset exposure analysis on the nine hazard data sets/zones (section 5.3.1 Exposure Analysis) and the three asset data sets: permanent population; critical facilities and primary infrastructure; and generalized occupancy and buildings (section 5.3.1 Exposure Analysis). Tables showing the results of this analysis are detailed in Appendix F.

Table 13 is a summary of the exposure of select assets to the three landslide types. We found approximately \$1 billion of land and buildings and almost 8,000 people are located on existing landslides.

Table 14 is a summary of exposure of select assets to the six landslide susceptibility classes from the deep and shallow susceptibility maps. We found approximately \$7.5 billion of land and buildings are located in and over 20,000 people live in high-susceptibility hazard zones for shallow and deep landslides in the study area.

Table 13. Summary of exposure of select assets to three landslide types.

Type	Permanent Population	Buildings	Building Value	Parcels	Land Value	Critical Facilities Parcels	Road, Total Miles	Electric Transmission Towers
Shallow Landslides	227	123	\$16,809,407	1,146	\$36,410,453	3	2	1
Deep Landslides	7,247	3,128	\$416,470,782	5,085	\$416,416,811	3	58	42
Fans	487	412	\$32,543,039	1,074	\$36,218,574	0	7	2

Table 14. Summary of the six landslide susceptibility hazard zones and study area wide exposure of select assets.

Hazard	Permanent Population	Buildings	Building Value	Parcels	Land Value	Critical Facilities Parcels	Road, Total Miles	Electric Transmission Towers
<i>Shallow Landslide Hazard</i>								
Low	253,824	140,848	\$20,922,093,084	121,188	\$12,127,096,572	228	1,626	590
Moderate	75,922	56,451	\$12,145,072,582	65,006	\$3,557,700,590	177	470	147
High	9,702	18,070	\$5,322,269,216	55,960	\$979,024,018	155	24	30
<i>Deep Landslide Hazard</i>								
Low	319,317	145,037	\$21,771,760,886	122,575	\$16,024,043,544	241	2,113	623
Moderate	9,360	6,043	\$721,424,575	10,298	\$574,759,967	11	105	57
High	10,580	5,145	\$690,387,089	7,051	\$610,167,445	5	87	85

6.7.2 Hazus-MH analysis results

To examine the estimated damage and losses from landslides triggered by an earthquake, we performed five different Hazus-MH analyses (Table 5):

- crustal M6.8 earthquake scenario: Portland Hills Fault – no landslides
- crustal M6.8 earthquake scenario: Portland Hills Fault – detailed landslides
- crustal M6.8 earthquake scenario: Portland Hills Fault – landslide hazard set to 9 out of 10
- Cascadia M9.0 earthquake scenario – no landslides
- Cascadia M9.0 earthquake scenario – detailed landslides

Detailed reports for each of the five analyses are provided in Appendix H. The results show that the earthquake-induced landslide hazard alone would result in total economic loss ranging from approximately \$290 million to over \$1 billion (Table 15). The Hazus-MH estimate for the replacement value for the study area is roughly \$38.8 bil-

lion (Appendix H). Hazus-MH estimates a replacement value for buildings at approximately \$31.5 billion, which is significantly more than the taxable improvements (building) value of \$22.8 billion we derived from tax lot data. (See Appendix F for details.) The reason for the difference in total building value between our database and the Hazus-MH database is unclear and points to the need to update the Hazus-MH standard inventory data with more accurate local data.

Total economic loss values are likely underestimates due to the low quality of the standard Hazus-MH asset data, especially the critical facilities and infrastructure data. However, the loss ratios are likely to be better estimates than the absolute numbers. For example, the total loss ratios found in this study (2% to 21%) are very close to the estimated commercial and residential lines of business loss ratios (1% to 30%) for a M7.9 event on the San Andreas Fault affecting the 19 counties in the San Francisco Bay area (RMS, 2006).

Table 15. Summary of Hazus-MH results for this study.

	Crustal M6.8 Earthquake—Portland Hills Fault				Cascadia M9.0 Earthquake		
	Landslides Not Included	Landslides Included, Detailed	Landslides Included, with Hazard Set to 9 out of 10	Landslides Only (Column 3 minus Column 2)	Landslides Not Included	Landslides Included, Detailed	Landslides Only (Column 7 minus Column 6)
Buildings—moderate damage	31,360	30,113	28,108	-1,247	6,026	6,261	235
Buildings—extensive damage	11,740	16,177	25,478	4,437	901	2,158	1,257
Buildings—destroyed	5,600	6,913	9,595	1,313	41	356	315
Total buildings—moderate to destroyed	48,700	53,203	63,181	4,503	6,968	8,775	1,807
Building damage count ratio	38%	41%	49%	—	5%	7%	—
Building loss (\$)	\$6,412,760,000	\$7,392,050,000	\$9,649,200,000	\$979,290,000	\$737,950,000	\$1,004,200,000	\$266,250,000
Building loss (\$) ratio	20%	23%	31%	—	2%	3%	—
Residents needing shelter	3,766	5,019	7636	1,253	176	469	293
Casualties (5 pm)*	4,282	4,513	5,097	231	159	214	55
Fatalities (5 pm)*	290	302	332	12	2	4	2
Total economic loss ratio	\$7,222,500,000	\$8,271,820,000	\$10,621,100,000	\$1,049,320,000	\$880,840,000	\$1,171,840,000	\$291,000,000
Total economic loss ratio	19%	21%	27%	—	2%	3%	—

*For an earthquake occurring at 5 pm; casualty and fatality values differ for different times during the day. See Appendix H.

The analysis estimates damage by landslides alone will result in roughly 4,503 buildings being moderately to completely damaged and 1,253 residents needing shelter (Table 15).

For comparison, Wang and Clark (1999) examined earthquake damage from a M8.5 Cascadia earthquake in Clackamas County and found 73 buildings would be moderately to completely damaged from earthquake shaking alone.

7.0 DISCUSSION AND CONCLUSIONS

Although we cannot predict when the next landslide events will occur or how big they will be, we were able to provide a detailed understanding of landslide events in the past (historic and prehistoric), the potential scale of a disaster, the areas more or less susceptible to future landslides, and an estimate of what the damage and losses might be. The main purpose of this project was to help communities in the study area become more resilient to landslide hazards by providing detailed, new digital databases describing the landslide hazards as well as community assets and the risk that exists where the two overlap.

Detailed results have been discussed in this report, and detailed data are provided in appendices and on map plates via GIS data. Three primary conclusions of the project are:

- Large, deep landslides are a primary threat in the study area, and asset exposure to these landslides is significant —more than 7,000 residents and more than 3,000 buildings.
- Historic landslide losses range from hundreds of thousands to millions of dollars in normal storm years to and tens of millions of dollars in severe storm years such as 1996.
- Damage and losses from landslides alone, induced by a local large crustal earthquake, may be in the range of \$1 billion, with ~4,500 buildings moderately to completely destroyed.

The next step is to work on landslide risk reduction. The three primary actions are: 1) awareness, 2) regulations, and 3) planning.

Making everyone aware of the hazard in their area is crucial to help them understand the associated danger and how they can prepare themselves. One of the main purposes of the new maps is to help accomplish education throughout northwestern Clackamas County. Once the hazard is understood better, the land owner can work on risk reduction. Fliers can be made available on web-

sites and/or distributed to help educate land owners of activities individuals can work on to reduce landslide risk. Examples of helpful flyers include Homeowners Guide to Landslides (Burns and others, n.d.) and DOGAMI fact sheet Landslide hazards in Oregon (DOGAMI, 2006).

It is also important for the public to be notified during times of increased landslide potential. Oregon currently has a landslide warning system operated in partnership by the NOAA National Weather Service, DOGAMI, ODOT, and OEM. NOAA initiates the system by sending out landslide watches, and the state agencies help citizens become aware of the heightened potential. In the future, this information could be streamlined to the local municipalities (county and cities) via RSS feeds and live web pages. During these periods of increased landslide potential, the public could then access hazard maps to find locations where this potential is most likely.

Because the exposure to large, deep landslides in the study area is significant and these landslides have a high potential to move again, the inventory and susceptibility maps produced as part of this project show areas of low, moderate, and high potential for landslides and are suited for use connected to a landslide ordinance or building code regulation. The maps could also be used in short- and long-term development planning and comprehensive planning and maintenance planning. Some planning results could result in avoidance in high hazard areas and even buyouts in very high or life-threatening areas. These large slides are often hard to mitigate and involve cooperation from several entities (city and land owners) as the slides can span entire neighborhoods. To reduce the likelihood of a slide reactivating, a public awareness campaign could be undertaken to educate homeowners and land owners about the landslide hazards in their areas and how to reduce their risk. Residents on mapped landslide areas should participate in a neighborhood risk reduction program where all affected land owners (city and public) help reduce to the overall risk. Risk reduction measures should include:

- minimizing irrigation on slopes;
- avoiding removing material from the base of slopes;
- avoiding adding material or excess water to top of slopes;
- draining water from surface runoff, down-spouts; and driveways well away from slope and into storm drains or natural drainages; and
- consulting an expert to conduct a site-specific evaluation if considering major construction.

8.0 ACKNOWLEDGMENTS

Funding for this project was provided in part by Clackamas County through Intergovernmental Agreement IGA 11-21-2011. Some funding in the IGA was provided by FEMA-OEM hazard mitigation planning grant DR-1824 and from cities (including Happy Valley, Lake Oswego, Wilsonville, and Oregon City) and Metro. We thank them and Dennis Sigrist at Oregon Emergency Management.

We also thank Jay Wilson and Steve Hanschka from Clackamas County. Finally, we thank DOGAMI staff who helped work on this project through technical assistance, review, and general assistance, especially Yumei Wang, Deb Schueller, and Ian Madin.

9.0 REFERENCES

- Baum, R. L., Galloway, D. L., and Harp, E. L., 2008, Landslide and land subsidence hazards to pipelines, U.S. Geological Survey, Open-File Report 2008-1164.
- Burns, S. F., Harden, T. M., and Andrew, C. J., [n.d.], Homeowner's guide to landslides: recognition, prevention, control, and mitigation: Portland, Oreg., Portland State University, and Federal Emergency Management Agency Region X, Bothell, Wash., 12 p. Web: <http://www.oregongeology.org/sub/Landslide/homeowners-landslide-guide.pdf>.
- Burns, W. J., 2007, Comparison of remote sensing datasets for the establishment of a landslide mapping protocol in Oregon: Vail, Colo., 1st North American Landslide Conference: Association of Environmental and Engineering Geologists, AEG Special Publication 23.
- Burns, W. J., 2008, Regional landslide hazard maps of the southwest quarter of the Beaverton quadrangle, West Bull Mountain Planning Area, Washington County, Oregon: Oregon Department of Geology and Mineral Industries, Open-File Report O-08-09, 17 p., scale 1:8,000.
- Burns, W. J., 2009, Landslide inventory maps for the Canby quadrangle, Clackamas, Marion, and Washington Counties, Oregon: Oregon Department of Geology and Mineral Industries, Interpretive Map 29, scale 1:8,000.
- Burns, W. J., and Madin, I. P., 2009, Protocol for inventory mapping of landslide deposits from light detection and ranging (lidar) imagery: Oregon Department of Geology and Mineral Industries, Special Paper 42, 30 p., geodatabase template.
- Burns, W. J., and Duplantis, S., 2010, Landslide inventory maps for the Lake Oswego quadrangle, Clackamas, Multnomah, and Washington Counties, Oregon: Oregon Department of Geology and Mineral Industries, Interpretive Map 32, scale 1:8,000.
- Burns, W. J., and Mickelson, K. A., 2010, Landslide inventory maps for the Oregon City quadrangle, Clackamas, Marion, and Washington Counties, Oregon: Oregon Department of Geology and Mineral Industries, Interpretive Map 30, scale 1:8,000.
- Burns, W. J., Mickelson, K. A., and Saint-Pierre, E. C., 2011, Statewide Landslide Information Database for Oregon, release 2 (SLIDO-2), Oregon Department of Geology and Mineral Industries, CD-ROM. Web: <http://www.oregongeology.org/sub/slido/>
- Burns, W. J., Mickelson, K. A., and Duplantis, S., 2012a, Landslide inventory maps for the Sandy quadrangle, Clackamas and Multnomah Counties, Oregon: Oregon Department of Geology and Mineral Industries, Interpretive Map 38, scale 1:8,000.
- Burns, W. J., Madin, I. P., Mickelson, K. A., and Duplantis, S., 2012b, Landslide inventory maps for the Gladstone quadrangle, Clackamas and Multnomah Counties, Oregon: Oregon Department of Geology and Mineral Industries, Interpretive Map 48, scale 1:8,000.
- Burns, W. J., Madin, I. P., Mickelson, K. A., Duplantis, S., and Jones, C. B., 2012c, Landslide inventory maps for the Damascus quadrangle, Clackamas and Multnomah Counties, Oregon: Oregon Department of Geology and Mineral Industries, Interpretive Map 49, scale 1:8,000.
- Burns, W. J., Mickelson, K. A., and Duplantis, S., 2012d, Landslide inventory maps for the Sherwood quadrangle, Clackamas, Marion, Washington, and Yamhill Counties, Oregon: Oregon Department of Geology and Mineral Industries, Interpretive Map 50, scale 1:8,000.
- Burns, W. J., Madin, I. P., Mickelson, K. A., and Duplantis, S., 2012e, Landslide inventory maps for the Redland quadrangle, Clackamas County, Oregon: Oregon Department of Geology and Mineral Industries, Interpretive Map 51, scale 1:8,000.
- Burns, W. J., 2012f, Landslide inventory maps for the Estacada quadrangle, Clackamas, Marion, and Washington Counties, Oregon: Oregon Department of Geology and Mineral Industries, Interpretive Map 52, scale 1:8,000.

- Burns, W. J., Madin, I. P., and Mickelson, K. A., 2012g, Protocol for shallow-landslide susceptibility mapping: Oregon Department of Geology and Mineral Industries, Special Paper 45.
- Das, B. M., 1994, Principles of Geotechnical Engineering, 3rd ed.: Boston, Mass., PWS Publishing, 672 p.
- FEMA (Federal Emergency Management Administration), 2011, Hazus®-MH 2.1, Multi-Hazard loss estimation methodology, software and technical manual documentation. Web: <http://www.fema.gov/media-library/assets/documents/24609?id=5120>
- FEMA, 2012a. Web: http://www.fema.gov/disasters/grid/state-tribal-government/88?field_disaster_type_term_tid_1=All
- FEMA, 2012b. Web: <http://www.fema.gov/national-flood-insurance-program-2/critical-facility>
- Giraud, R.E., and Shaw, L. M., 2007, Landslide susceptibility map of Utah: Utah Geological Survey, Map 228, 11 p., 1 pl., scale 1:500,000, compact disk. Web: <http://geology.utah.gov/online/m/m-228.pdf>
- Hofmeister, R. J., 2000, Slope failures in Oregon: GIS inventory for three 1996/97 storm events: Oregon Department of Geology and Mineral Industries, Special Paper 34, 20 p., 1 CD-ROM.
- Lewis, D., 2007, Statewide seismic needs assessment: implementation of Oregon 2005 Senate Bill 2 relating to public safety, earthquakes, and seismic rehabilitation of public buildings: Oregon Department of Geology and Mineral Industries, Open-File Report O-07-02, 140 p.
- Ma, L., Madin, I. P., Olson, K. V., Watzig, R. J., Wells, R. E., Niem, A. R., and Priest, G. P. (compilers), 2009, Oregon geologic data compilation [OGDC], release 5 (statewide): Oregon Department of Geology and Mineral Industries, CD-ROM.
- Ma, L., Madin, I. P., Duplantis, S., and Williams, K. J., 2012, Lidar-based surficial geologic map and database of the greater Portland area, Clackamas, Columbia, Marion, Multnomah, Washington, and Yamhill Counties, Oregon, and Clark County, Washington: Oregon Department of Geology and Mineral Industries, Open-File Report O-12-02, 30 p., scale 1:63,360.
- Madin, I. P., and Burns, W. J., 2013, Ground motion, ground deformation, tsunami inundation, coseismic subsidence, and damage potential maps for the 2012 Oregon Resilience Plan for Cascadia Subduction Zone Earthquakes: Oregon Department of Geology and Mineral Industries, Open-File Report O-13-06, 36 p.
- Metro (Portland, Oregon, metropolitan area regional government), 2013, Regional Land Information System (RLIS) GIS database: Portland, Oreg., Metro Data Resource Center. Web: <http://web.multco.us/gis/metros-regional-land-information-system-rlis>
- Risk Management Solutions, Inc., 2006, The 1906 San Francisco earthquake and fire: perspectives on a modern Super Cat. Web: http://www.rms.com/publications/1906_SF_EQ.pdf
- Schlicker, H. G., and Finlayson, C. T., 1979, Geology and geological hazards of northwestern Clackamas County, Oregon: Oregon Department of Geology and Mineral Industries, Bulletin B-99, 79 p., scale 1:24,000.
- Schulz, W. H., 2007, Landslide susceptibility revealed by lidar imagery and historical records: Engineering Geology, v. 89, p. 67–87.
- Sidle, R. C., and Ochiai, H., 2006, Landslides: processes, prediction, and land use: Washington, D.C., American Geophysical Union, 312 p.
- Sleeter, R., and Gould, M., 2007, Geographic information system software to remodel population data using dasymetric mapping methods: U.S. Geological Survey Techniques and Methods 11-C2, 15 p. Web: <http://pubs.usgs.gov/tm/tm11c2/>
- Soeters, R., and van Westen, C. J., 1996, Slope stability analysis, in Turner, A. K., and Schuster, R. L., eds., Landslides: investigation and mitigation: Transportation Research Board, National Research Council, Special Report 247, Chap. 8, p. 129–177.
- Turner, A. K., and Schuster, R. L., eds., 1996, Landslides: investigation and mitigation: Transportation Research Board, National Research Council, Special Report 247, 673 p.
- Wang, Y., and Clark, L., 1999, Earthquake damage in Oregon: preliminary estimates of future earthquake losses: Oregon Department of Geology and Mineral Industries, Special Paper 29, 59 p.
- Wilson, R. C., and Keefer, D. K., 1985, Predicting areal limits of earthquake-induced landsliding, in Ziony, J. I., ed., Evaluating earthquake hazards in the Los Angeles region—an earth-science perspective: U.S. Geological Survey Professional Paper 1360, p. 316–345.